ACS Infectious Diseases

Article

Cite This: ACS Infect. Dis. 2018, 4, 158−174

pubs.acs.org/journal/aidcbc

C8-Linked Pyrrolobenzodiazepine Monomers with Inverted Building Blocks Show Selective Activity against Multidrug Resistant Gram-Positive Bacteria

Paolo Andriollo,[†,⊥] Charlotte K. Hind,[‡,⊥] Pietro Picconi,[†] Kazi S. Nahar,[†] Shirin Jamshidi,[†] Amrit Varsha,[†] Melanie Clifford,[‡] J. Mark Sutton,[*,‡] and Khondaker Miraz Rahman[*,†]

[†]Institute of Pharmaceutical Science, King's College London, 150 Stamford Street, London SE1 9NH, United Kingdom

[‡]National Infections Service, Public Health England, Manor Farm Road, Porton Down, Salisbury SP4 0JG, United Kingdom

Supporting Information

ABSTRACT: Antimicrobial resistance has become a major global concern. Development of novel antimicrobial agents for the treatment of infections caused by multidrug resistant (MDR) pathogens is an urgent priority. Pyrrolobenzodiazepines (PBDs) are a promising class of antibacterial agents initially discovered and isolated from natural sources. Recently, C8-linked PBD biaryl conjugates have been shown to be active against some MDR Gram-positive strains. To explore the role of building block orientations on antibacterial activity and obtain structure activity relationship (SAR) information, four novel structures were synthesized in which the building blocks of previously reported compounds were inverted, and their antibacterial activity was studied. The compounds showed minimum inhibitory concentrations (MICs) in the range of 0.125−32 μg/mL against MDR Gram-positive strains with a bactericidal mode of action. The results showed that a single inversion of amide bonds reduces the activity while the double inversion restores the activity against MDR pathogens. All inverted compounds did not stabilize DNA and lacked eukaryotic toxicity. The compounds inhibit DNA gyrase *in vitro*, and the most potent compound was equally active against both wild-type and mutant DNA gyrase in a biochemical assay. The observed activity of the compounds against methicillin resistant *S. aureus* (MRSA) strains with equivalent gyrase mutations is consistent with gyrase inhibition being the mechanism of action *in vivo*, although this has not been definitively confirmed in whole cells. This conclusion is supported by a molecular modeling study showing interaction of the compounds with wild-type and mutant gyrases. This study provides important SAR information about this new class of antibacterial agents.

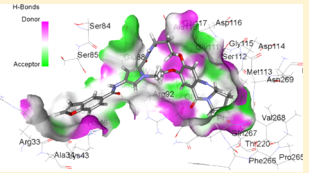

KEYWORDS: *antimicrobial resistance, medicinal chemistry optimization, minimum inhibitory concentration, pyrrolobenzodiazepine, ESKAPE pathogens*

The resistance of pathogens to antibacterial agents has become a major global concern. Multidrug resistant (MDR) bacteria cause many common and severe infections for which treatment is increasingly becoming difficult or in some cases impossible.[1] The spread of healthcare-associated infections and associated antimicrobial resistance is facilitated by interspecies gene transmission, poor sanitation, and hygienic conditions, along with the increasing frequency of global travel, trade, and disease transmission.[2] Of great concern among all the bacteria that are developing resistance is a group of pathogens termed the ESKAPE pathogens,[3] which are characterized by the rapid acquisition of resistance to multiple classes of antibiotic (with resistance to 3 or more classes referred to as multidrug resistance). These species are primarily associated with nosocomial infections especially among immunocompromised patients,[4] and this also has an additional economic impact upon the healthcare system.[1,5] Although the measurement of additional costs is complicated,[6] the estimated economic impact for the U.S. economy is reported to be higher than $20 billion in direct annual healthcare costs.[7]

In the last 30 years, no major classes of broad spectrum antibiotics have been introduced to the market, and recently approved agents like linezolid (2000), daptomycin (2003), and retapamutilin (2007) are active only against Gram-positive pathogens.[8] A recent report from the World Health Organization has highlighted the limited number of drugs in the pipeline with only a few molecules in phase 2 and 3 of clinical development against ESKAPE pathogens; these are predominantly focused on Gram-positive species or are iterations of existing drugs (notably β-lactamase inhibitor combinations). This highlights the need to identify and evaluate new therapeutic options and/or to modify existing chemical scaffolds to obtain antibiotics with improved properties,[10] and a number of agents developed through this approach are currently undergoing clinical trials.[9]

Applying the same principle, we selected the pyrrolobenzodiazepines (PBDs) as a relatively unexplored chemical scaffold to generate new antibacterial compounds with improved bioactivity and elucidate the structure activity relationship (SAR) of C8-linked PBDs. PBDs are naturally occurring molecules produced by *Streptomyces* bacteria whose family

Received: August 22, 2017
Published: December 20, 2017

DOI: 10.1021/acsinfecdis.7b00130
ACS Infect. Dis. 2018, 4, 158−174

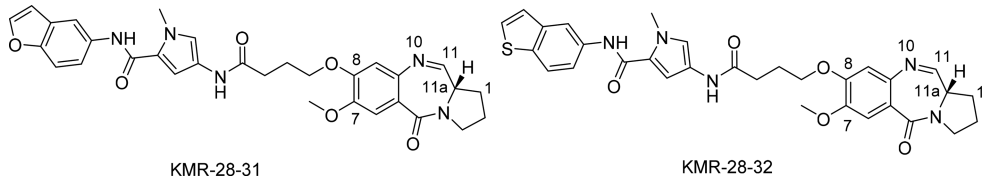

Figure 1. Structure of KMR-28-31 (**27**, PBD-Py-Bzf) and KMR-28-32 (**30**, PBD-Py-Bzt), previously reported C8-benzofused PBDs with antistaphylococcal activity (MIC $\leq$ 0.125 μg/mL).

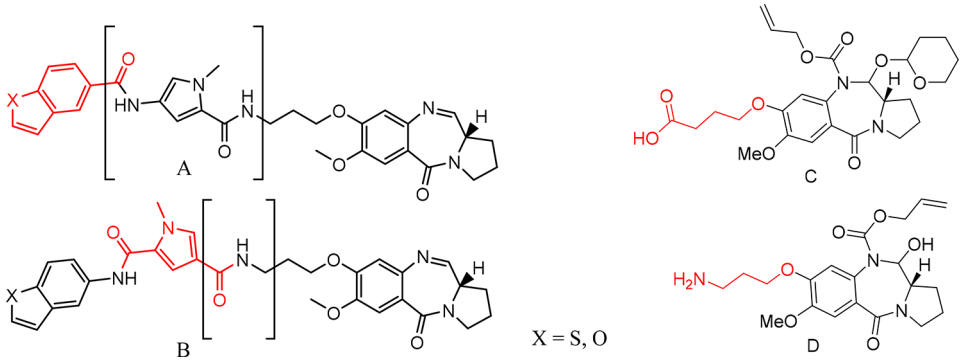

Figure 2. (A, B) Structures showing (in brackets) the reverse moieties and (in red) the different building blocks from the reference compounds. (C) Traditional PBD core with 4C-acid linker. (D) New PBD core with 4C-amine linker.

members include anthramycin and tomaymycin.[11,12] PBDs are a class of sequence-specific DNA minor groove binding agents that are selective for GC-rich sequences, which have been evaluated as potential chemotherapeutic agents in recent years.[13] PBDs have a chiral center at their C11a(*S*)-position which provides an appropriate 3D shape for them to fit securely within the DNA minor-groove. They also possess a "soft" electrophilic imine moiety at their N10−C11 position which can form an aminal linkage between their C11-position and the C2−NH_2 group of a guanine base only when the molecule is secure within the minor groove.[14,15] Anthramycin was the first naturally derived PBD, initially discovered and isolated in 1963 from *Streptomyces* and *Micrococci* bacteria,[16] and later many other natural and synthetic PDBs followed. Naturally occurring PBDs such as anthramycin, tomaymycin, neothramycin, and sibiromycin form adducts that span three base pairs, with guanine in the central position,[17,18] and their preferred binding site is 5′-AGA-3′,[19] although more recent data suggest that they have a kinetic preference for 5′-Py-G-Py-3′ sequences.[20] PBD monomers can recognize and bind to specific sequences of DNA and therefore have the potential to act as competitive inhibitors of transcription factors. Considering their mechanism of action, PBDs have been extensively studied as anticancer agents but relatively unexplored as antibacterial agents.[21−24] Different studies showed the possibility of synthesizing PBD analogues characterized by their high selectivity for particular DNA sequences, by modifying the C8 position substituent.[25,26] For example, PBD−biaryl conjugates, a subclass of monomers with C8-subunits, have shown preferences for GC sequences.[27] Molecules belonging to this subclass have been demonstrated to be well tolerated in mice at high concentrations, and molecular dynamics simulations indicate that they are easily accommodated within the minor groove causing little distortion to the DNA structure.

We previously studied numerous PBD−biaryl conjugated structures and identified some characteristics that are important for optimal antibacterial activity against Gram-positive pathogens.[24] Among the compounds studied, we selected two compounds which showed excellent antibacterial activity against MDR Gram-positive pathogens (minimum inhibitory concentration (MIC) range: 0.003−0.125 μg/mL) for our investigation. The first compound is a PBD-Py-Bzf (Py = pyrrole, Bzf = benzofuran) conjugate, while the second structure was a PBD-Py-Bzt (Bzt = benzothiophene) (Figure 1) conjugate. Starting from these two molecules, we designed four new molecules with a different orientation of the building blocks constituting the C8 lateral chain. It has been reported in the literature that the standard orientation of the amide bonds provide additional hydrogen bond contact with the minor groove of DNA, and inversion of the amide linkage should result in loss of these contacts and reduced binding to DNA.[23,25] There is a positive correlation between DNA binding and eukaryotic toxicity of PBD monomers, and a reduction in binding should result in reduction or loss of toxicity. First, we wanted to investigate the antibacterial activity of the derivatives characterized by the inversion of the amide linkage between *N*-methylpyrrole and the alkyl spacer and later the derivatives with both the reverse *N*-methylpyrrole and the amide bonds between the building blocks (Figure 2) and obtain compounds with reduced eukaryotic toxicity. To achieve the synthesis of these new PBD-C8-benzofused conjugates, we needed a new PBD core with a 4C−NH_2 linker in place of traditional 4C−COOH linker. Tiberghien et al. reported the use of this functionality in 2008[28] for the synthesis of PBD dimers, but in this work, for the first time, it was used for the synthesis of C8-linked PBD monomers; the synthesized compounds are the first examples of C8-linked PBD monomers with an inverted amide linkage between the 4C-spacer and the heterocyclic building blocks. Moreover, from a synthetic chemistry point of view, this modification allowed us to avoid the protection of the hydroxyl group at C11, otherwise necessary to prevent the racemization of (*S*) C11a observed in the previous synthesis during the basic methyl ester hydrolysis employed in C8-PBD monomer synthesis.[23]

The newly synthesized compounds were tested against susceptible and MDR Gram-positive bacterial strains. The

DOI: 10.1021/acsinfecdis.7b00130
ACS Infect. Dis. 2018, 4, 158−174

Scheme 1. Synthesis of PBD Acid Core 9

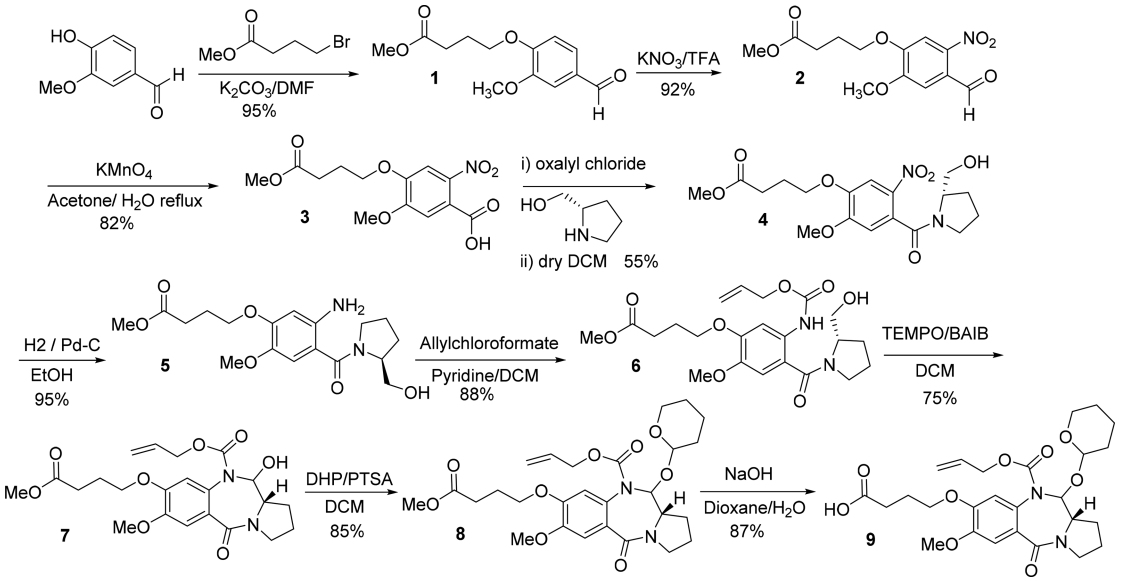

Scheme 2. Synthesis of PDB Amino Core 18

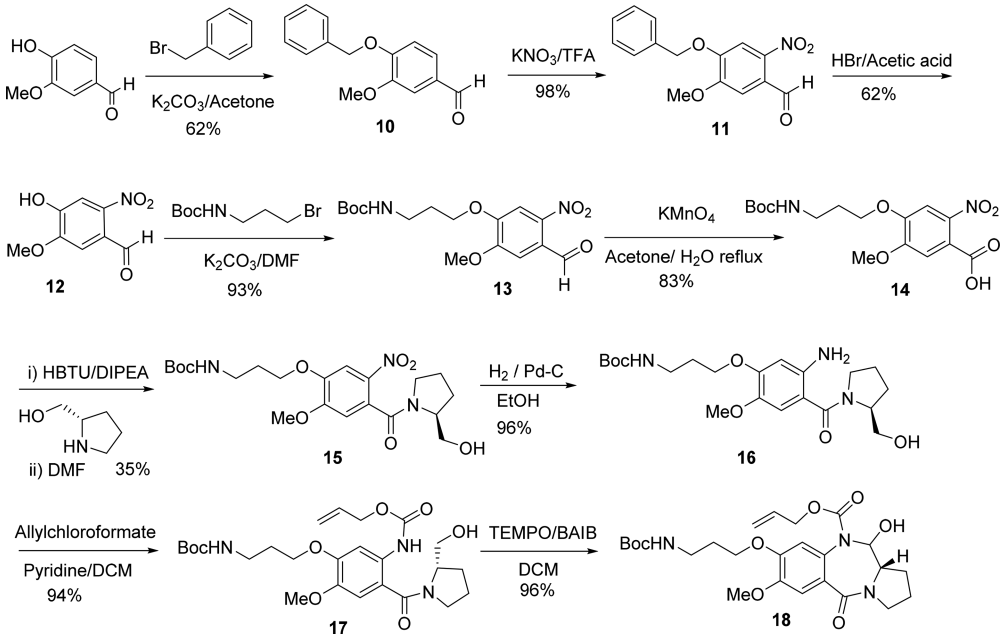

compounds were also tested in a fluorescence resonance energy transfer (FRET) based DNA melting assay, to evaluate the effect of inverse orientation on the DNA binding ability of the compounds, and against mammalian cell lines to assess their selectivity for prokaryotic cells. The mechanisms of action of the compounds were studied initially by an *in silico* screening against bacterial targets, followed by a biochemical assay against the wild-type and mutant target identified by the *in silico* study. Finally, molecular modeling experiments were performed to rationalize the obtained biological results.

RESULTS AND DISCUSSION

Chemistry. Both the synthetic strategies followed for the synthesis of the core bearing the 4C−COOH (Scheme 1) and the core bearing 4C−NH_2 functionality are based on the previously reported Thurston/Rahman approach.[23] The PBD core used to synthesize the final compounds with standard orientation was obtained as Alloc-THP-protected PBD unit (**9**). Briefly, vanillin was alkylated with methyl 4-bromobutyrate employing K_2CO_3 in DMF providing the ester derivative **1** after precipitation. Subsequently, **1** underwent a selective nitration reaction using KNO_3/TFA to give **2** in good yield after an aqueous workup. The nitrobenzaldehyde derivative **2** was then oxidized to the carboxylic acid intermediate **3** using $KMnO_4$. The key intermediate **4** was obtained by amide coupling between **3**, which had been activated to the corresponding acid chloride by treatment with oxalyl chloride, and optically pure (*S*)-pyrrolidine methanol. Reduction of the nitro derivative **4** to the corresponding amino derivative **5** was accomplished with Pd/C in a Parr hydrogenator system at 40 psi, followed by Alloc protection giving **6** in good yield after purification by column chromatography. The Alloc-protected PBD ring system

DOI: 10.1021/acsinfecdis.7b00130
ACS Infect. Dis. 2018, 4, 158−174

7 was then obtained by oxidative cyclization using the BAIB/TEMPO oxidizing system. In order to prevent racemization at the C11*a* position of the PBD ring system, which occurs under alkaline conditions, the alcohol derivative 7 was protected with a THP ether giving 8. The final Alloc-THP-protected PBD capping unit 9 was obtained via hydrolysis of the methyl ester using 0.5 M NaOH aqueous solution.

The synthetic strategy to obtain the C8-linked PBDs with inverted amide bonds (Scheme 2) involved protection of the reactive amino group on the 4C-spacer to avoid side reactions, and the reaction steps were adjusted to take this modification into account. Particularly, acidic conditions were avoided after the introduction of the Boc-protected amine side chain. To obtain the type 2 core, vanillin was coupled with benzyl bromide under alkaline condition giving the ether derivative 10 after recrystallization. This additional step allowed the selective nitration that led to 11 with a good yield. The benzyl group was then removed with concentrated HBr in acetic acid to afford the nitro-vanillin derivate 12. The amide coupling reaction with (*S*)-pyrrolidine methanol to obtain 15 was performed using 2-(1*H*-benzotriazol-1-yl)-1,1,3,3-tetramethyluronium hexafluorophosphate (HBTU) and *N*,*N*-diisopropylethylamine (DIPEA) rather than oxalyl chloride to avoid the generation of acid. The final Alloc-protected PBD capping unit was obtained via the deprotection of the amino group by TFA in DCM, just before the coupling with the selected tail.

The synthesis of the C8-side chains was achieved by amide coupling between the selected building blocks (Scheme 3). An

Scheme 3. Generic Amide Coupling Reactions in the Synthesis of Benzofused-*N*-Methylpyrrole Intermediates

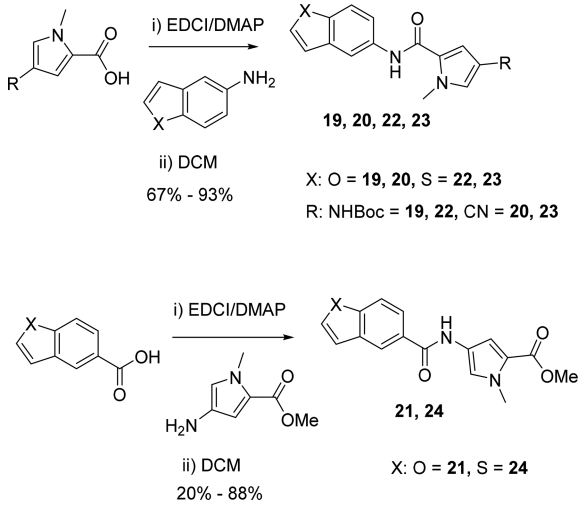

EDCI/DMAP reagents system was used for the activation of the acid, leading to intermediate 19 to 24 with variable yield (20% to 93%). Nitrile groups of 20 and 23 were hydrolyzed by refluxing in dioxane in a strongly acidic environment (with the presence of H_2SO_4) to give 25 and 26 after purification by column chromatography.

The last step in the synthesis of the C8-linked benzofused-*N*-methylpyrrole PBD derivatives consisted of several sequential passages. At first, when it was necessary, the capping units were deprotected. Methyl esters of derivatives 21 and 24 were hydrolyzed under basic conditions (in a NaOH aqueous solution), leading to the acid compounds, while the amino groups on 19 and 22 were deprotected in an acidic environment (TFA in DCM). Subsequently, the PBD core and the benzofused-*N*-methylpyrrole tails were connected through an amide coupling reaction. Once again, the EDCI/DMAP system was used to carry out acid activation and coupling. Finally, the conjugated products were deprotected with pyrrolidine and $Pd(PPh_3)_4$ in DCM, affording the final compounds 27, 28, 29, 30, 31, and 32 (Scheme 4). The final deprotection was common to all the products regardless of the presence of THP protection, and both the protected and the final PBD imine conjugates were purified by column chromatography.

Evaluation of DNA Binding Ability of the Synthesized Compounds. The ability of compounds 27, 28, 29, 30, 31, and 32 to bind and stabilize the DNA was evaluated using a FRET based DNA melting assay[29] to understand the effect of building block orientation on the DNA binding ability of the compounds. The compounds were tested using two fluorophore-labeled oligonucleotide sequences (Sequence F1: 5′-FAM-TAT-ATA-TAG-ATA-TTT-TTT-TAT-CTA-TAT-ATA-3′-TAMRA and Sequence-F2: 5′-FAM-TAT-AGA-TAT-AGA-TAT-TTT-ATA-TCT-ATA-TCT-ATA-3′-TAMRA, where FAM is 6-carboxyfluorescein and TAMRA is 5-carboxytetramethylrhodamine). Netropsin, a known DNA minor groove binder, was used as a positive control. The result of the assay is reported in Table 1. Previously reported C8-PBD conjugates 27 and 30 and control compound netropsin showed notable stabilization of both DNA sequences at 1 μM, but the C8-PBD compounds with inverted building blocks, 28, 29, 31, and 32 did not stabilize the DNA sequence, with ΔT_m values <1 °C at 1 μM concentration (drug/DNA ratio 5:1). The result suggests the inversion of single or both amide bonds reduced the ability of these compounds to interact with and stabilize the DNA sequences.

Evaluation of Eukaryotic Toxicity. The inability of the inverted C8-PBD conjugates to stabilize DNA sequences suggested the compounds may show reduced toxicity against eukaryotic cell lines, as DNA stabilization has been associated with cytotoxicity for PBD-type covalent minor groove binders.[30] The eukaryotic cytotoxicity of the synthesized compounds was tested against the cervical cancer cell line HeLa and the nontumor lung fibroblast WI38 using an MTT assay.[31] The original C8-PBD benzofused conjugates 27 and 30 showed very potent cytotoxicity against the HeLa cell line (Figure 3) with only 25% and 32% cells viable after 24 h. The compounds showed slightly less toxicity against the nontumor cell line WI 38 with 42% and 47% cells viable after 24 h. However, the inverted compounds 28, 29, 31, and 32 showed notably less toxicity against both HeLa and WI38 cell lines. In the case of the inverted compounds, >70% of cells were viable after 24 h of treatment with the molecules. This lack of toxicity was in line with the DNA binding ability of the compounds, and this is consistent with previous reports that PBDs exert their cytotoxicity by alkylating and stabilizing DNA sequences.[32]

Microbiological Evaluation. The inverted amide compounds and the parent compounds were tested against a selected panel of Gram-positive bacteria to assess their antibacterial activity (Table 2). The Gram-positive panel was comprised of *Staphylococcus aureus* and *Enterococcus spp.* strains, which comprise the "S" and the "E" from the ESKAPE pathogens acronym. The strains used were methicillin sensitive *S. aureus* (MSSA) strain ATCC 9144, two methicillin resistant *S. aureus* (MRSA) strains, EMRSA-15 (strain HO 5096 0412) and EMRSA-16 (strain MRSA 252), vancomycin sensitive

DOI: 10.1021/acsinfecdis.7b00130
ACS Infect. Dis. 2018, 4, 158−174

Scheme 4. Synthesis of Standard and Inverted Orientation Benzofused-*N*-Methylpyrrole PBD Derivatives

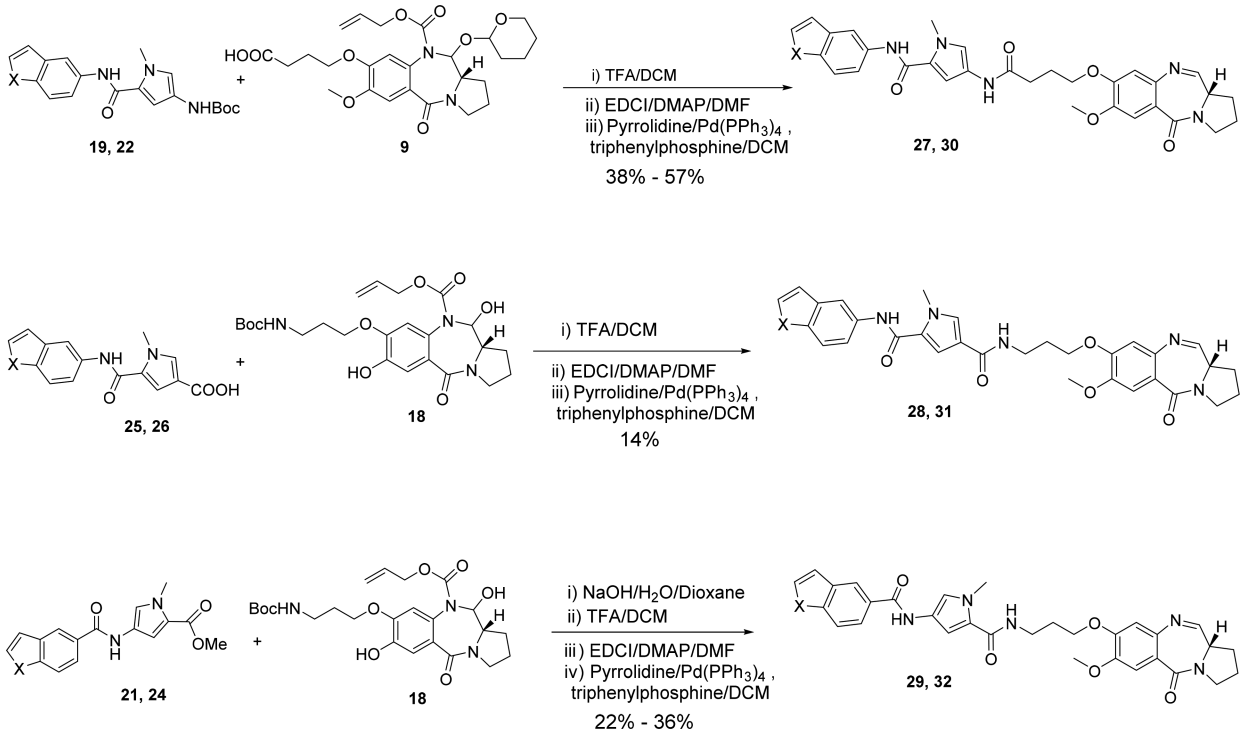

Table 1. DNA Duplex Stabilization for Natural and Inverted C8-PBD Compounds[a]

	ΔT_m at 1 μM	
compounds	sequence F1	sequence F2
27	20.8 ± 0.2	9.5 ± 0.5
28	0.0 ± 0.2	0.4 ± 0.1
29	0.1 ± 0.1	0.5 ± 0.3
30	21.7 ± 0.2	11.1 ± 0.9
31	0.2 ± 0.1	0.5 ± 0.1
32	0.4 ± 0.1	0.9 ± 0.1
netropsin	13.8 ± 0.3	11.0 ± 0.2
ciprofloxacin	0.0 ± 0.4	0.2 ± 0.3

[a] ΔT_m values are reported in the table in C° in comparison to the control. Assay conducted in triplicate.

E. faecalis (VSE), strain NCTC 755, vancomycin resistant *E. faecalis* (VRE, vancomycin resistant *Enterococci*), strain NCTC 12201, and vancomycin resistant *E. faecium* (VRE), strain NCTC 12204. As expected, compound **27** showed good antibacterial activity with MICs lower than 0.125 μg/mL against all Gram-positive strains tested. Surprisingly, the inversion of one amide linkage in compound **28** resulted in a considerable loss of activity with an MIC of 2 μg/mL against VRE strains and 16 μg/mL against VSE and MSSA strains. The drop in activity was particularly surprising against MRSA strains, with an MIC higher than 32 μg/mL. Interestingly, compound **29**, characterized by the inversion of both the amide linkages and the *N*-methylpyrrole building block, presented a better antibacterial profile than **28**. Although it was found to be less potent than **27**, compound **29** maintained moderate activity against the bacterial strains with MICs between 0.5 and 4 μg/mL. The observations made for the benzofuran series of C8-PBD conjugates were further confirmed by evaluating the C8-benzothiophene series of inverted and parent PBD compounds (Table 2). Compound **32** showed antibacterial

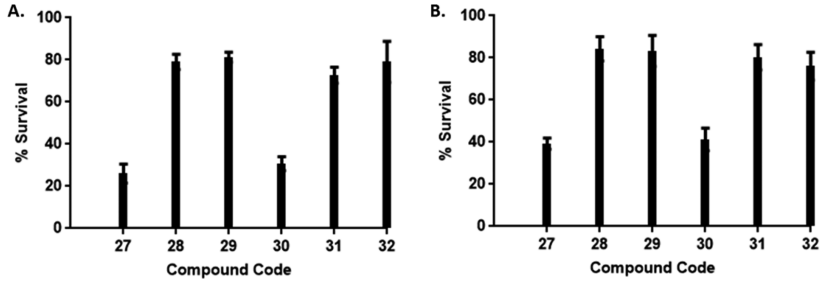

Figure 3. Eukaryotic toxicity of the C8-benzofused PBDs with natural and inverted building blocks at 25 μM after 24 h of incubation against (A) cervical cancer cell line HeLa and (B) nontumor lung fibroblast WI38.

DOI: 10.1021/acsinfecdis.7b00130
ACS Infect. Dis. 2018, 4, 158−174

Table 2. Minimum Inhibitory Concentrations of C8-PBD Benzofused Analogues with Natural and Inverted Building Blocks against Gram-Positive Strains and IC_{50}s, Against Eukaryotic Cells

	Gram-positive strains MIC (μg/mL)						IC_{50} (μg/mL)	
	VRE		VSE	MRSA		MSSA		
compound	NCTC 12201	NCTC 12204	NCTC 775	EMRSA 15	EMRSA 16	ATCC 9144	WI38	HeLa
27	≤0.125	≤0.125	≤0.125	≤0.125	≤0.125	≤0.125	0.14	0.03
28	2	2	16	>32	>32	16	>28.4	>28.4
29	0.5	1	4	2	4	2	>28.4	>28.4
30	≤0.125	≤0.125	≤0.125	≤0.125	≤0.125	≤0.125	0.07	0.03
31	2−4	≤0.125	1	>32	>32	16	>28.4	>28.4
32	≤0.125	≤0.125	≤0.125	>32	>32	16	>28.4	>28.4
Cipro	0.5	2	1	32	32	≤0.125	>28.4	>28.4

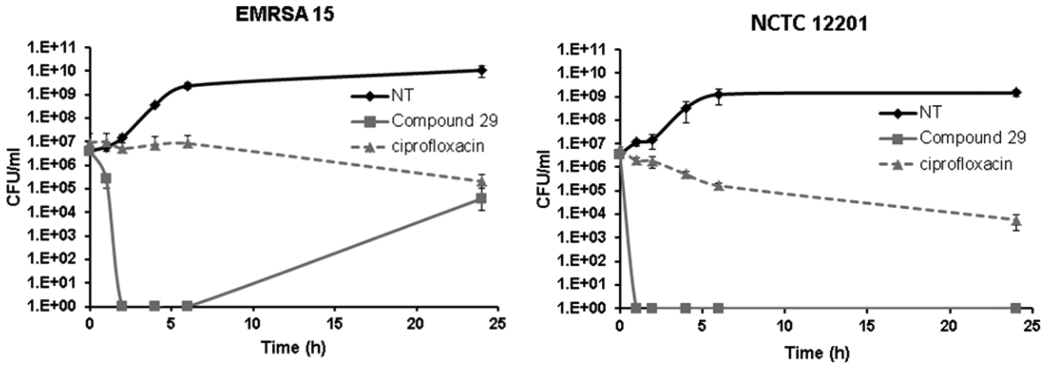

Figure 4. Response of EMRSA-15 and VRE-12201 strains to treatment with suprainhibitory concentrations (4× MIC) of compound **29**.

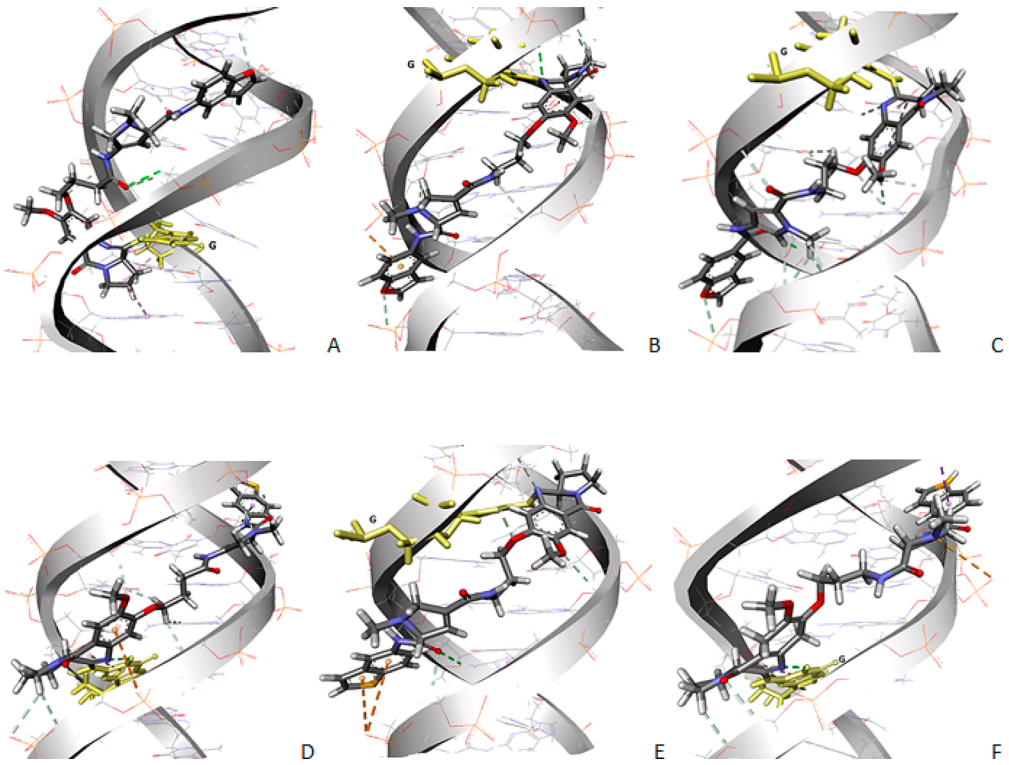

Figure 5. Covalent interactions between a random sequence of DNA and compounds **27** (A), **28** (B), and **29** (C) in the top panel and **30** (D), **31** (E), and **32** (F) in the lower panel. All compounds lay along the minor groove of DNA and form covalent interaction to the exocyclic N_2 atom of NH_2 group of a guanine (in yellow sticks) with their C11 atom present in the C═N imine bond.

activity comparable to previously reported compound **30** against *Enterococci* strains with MICs lower than 0.125 μg/mL. However, a drop in activity was observed against *S. aureus* strains with MICs higher than 32 μg/mL against MRSA and of 16 μg/mL against MSSA. Compound **31** showed antibacterial activity similar to **32** against *S. aureus* strains but generally

DOI: 10.1021/acsinfecdis.7b00130
ACS Infect. Dis. 2018, 4, 158−174

showed higher MICs against other strains. Overall, the inverted C8-linked benzothiophene PBD compounds showed better antibacterial activity against *Enterococcus* strains compared to the benzofuran compounds, while among the four newly synthesized compounds, the inverted benzofuran derivative **29** was found to be most active against *S. aureus* strains.

The mode of action of compound **29** was explored using time-kill assays. One MRSA (EMRSA-15) and one VRE (NCTC 12201) strain were treated with compound **29** at 4 × MIC for 24 h, and cell counts were elucidated at specified time points. The results show a rapidly bactericidal mode of action in both strains for compound **29**, with cell counts falling below the limit of detection within 2 h, while the control antibiotic ciprofloxacin displayed a bacteriostatic mode of action (Figure 4). Although a small population of cells was detected after 24 h of treatment with compound **29** in EMRSA-15 (in two of three replicate experiments), no resistance to the compound was detected in this population (assessed by determining the MIC of surviving cells), and as such, they most likely represent a persistor population. This is observed in EMRSA15 (fluoroquinolone resistant) but not in strain NCTC12201 (fluoroquinolone sensitive), although the role of fluoroquinolone resistance in persistor survival in these assays is unproven.

In Silico DNA Interaction Study. In order to rationalize the obtained results, a molecular modeling study was carried out using three random sequences of DNA: AT-rich Seq-1 (5′-TATATAAGATATATATA-3′), GC-rich Seq-2 (5′-TAGCTAGCTAGCTAGCG-3′), and mixed AT/GC Seq-3 (5′-GCGCGCGCGCGGCGCGC-3′). Covalent molecular docking between the N atom of the NH_2 group of guanine and the C11 atom of the C═N imine bond in PBDs showed favorable complexes with good affinities between PBDs and DNA. As PBDs are known to work by interacting with the DNA minor groove, we calculated the relative binding free energy of the DNA−compound complex (Figure 5) using molecular dynamics simulations followed by Molecular Mechanics-Poisson Boltzmann Surface Area (MM-PBSA)/Molecular Mechanics-Generalized Born Surface Area (MM-GBSA) calculations (Table 3). These models showed favorable energy values of ΔG_{GB} and ΔG_{PB} for the reference compounds in all three sequences while the results for the inverted compounds (**28**, **29**, **31**, and **32**) were considerably lower than the parent compounds **27** and **30**. The modeling study supported the lack of DNA stabilization observed in the FRET melting study and the lack of eukaryotic toxicity. Overall, a positive correlation between the free energy of binding and antibacterial activity was observed suggesting that DNA binding plays a role in the antibacterial potency of these compounds.

Mechanistic Evaluation. As the inverted C8-analogues did not stabilize DNA sequences and were nontoxic to eukaryotic cells, the mechanism of action of these molecules is likely to be DNA independent. To explore this further, we carried out an *in silico* docking campaign with known bacterial targets (ESI) to get an indication of the mechanism of action of these inverted pyrrolobenzodiazepines. Among the targets studied, the inverted compound **29** interacted with the ligand binding domain of DNA gyrase and showed excellent affinity toward both subunits of bacterial DNA gyrase. The best pose of compound **29** with the bacterial gyrase from *Staphylococcus aureus* (PDB ID 2XCT) gave a CHEM Score of 21.68 and affinity of −29 (kcal/mol) for subunit 1 of gyrase A and a CHEM Score of 23.29 and affinity of −30 (kcal/mol) for subunit 2 of gyrase A (Figure 6 and Table S2). The 2D models

Table 3. Energy Values Calculated Using the Poisson Boltzmann Model and Generalized Born Model and Expressed as kcal/mol for Each DNA−Compound Complex

complex	ΔG_{GB} (kcal/mol)	ΔG_{PB} (kcal/mol)
Seq1-**27**	−39	−40
Seq1-**28**	−34	−35
Seq1-**29**	−33	−35
Seq1-**30**	−42	−43
Seq1-**31**	−36	−39
Seq1-**32**	−35	−38
Seq2-**27**	−38	−39
Seq2-**28**	−37	−38
Seq2-**29**	−36	−37
Seq2-**30**	−42	−43
Seq2-**31**	−38	−40
Seq2-**32**	−37	−40
Seq3-**27**	−41	−43
Seq3-**28**	−38	−39
Seq3-**29**	−37	−39
Seq3-**30**	−43	−45
Seq3-**31**	−37	−39
Seq3-**32**	−38	−39

shown in Figure 6C suggest compound **29** forms three conventional hydrogen bonds with serine 98, arginine 92, and glutamine 95 of the subunit 1 of DNA gyrase A. Other key interactions are reported in Table S4. Similarly, compound **29** also forms three conventional hydrogen bonds with serine 85, arginine 92, and serine 98 of the subunit 2 of gyrase A (Figure 6D). A number of hydrophobic and electrostatic interactions with different amino acids from subunits of gyrase A were also observed (Table S5). The interaction of **29** with the ligand binding site of gyrase A suggests the antimicrobial activity is due to the inhibition of gyrase A by directly interacting with the enzyme and not due to its ability to associate with DNA.

The *in silico* observation was validated by carrying out a DNA gyrase inhibition assay using a commercial *S. aureus* gyrase supercoiling high throughput plate assay (#SATRG01) kit obtained from Inspiralis (Norwich, UK) (Figures 7 and S4). Compound **29** inhibited wild-type gyrase isolated from *S. aureus* with an IC_{50} of 0.95 ± 0.30 μg/mL which is significantly ($P < 0.05$) better than ciprofloxacin which inhibited the wild-type gyrase with an IC_{50} of 2.85 ± 1.80 μg/mL. Surprisingly, compounds **27** and **30** also showed comparable IC_{50}'s, 1.65 ± 0.68 and 2.28 ± 0.98 μg/mL, respectively, against wild-type gyrase (Figure 7). There was no statistically significant difference between the IC_{50} of compounds **27**, **29**, and **30**. This data does not provide a clear differential in gyrase inhibition between compounds that stabilize DNA (**27** and **30**) and may inhibit gyrase, a DNA associated enzyme, and compounds that have not shown DNA stabilization (**29** and ciprofloxacin, Table 1), where we would infer direct inhibition by gyrase binding. Competition assays were used to try and define the basis of the interaction. However, no clear answer could be obtained, as doubling the concentration of enzyme in the gyrase assays reduced the inhibition caused by compound **29** and ciprofloxacin but not compound **30**, which supports our inference, but a reduction in inhibition was also observed for compound **27** which could not be explained (Figure S5).

One of the most common mutations found in fluoroquinolone resistant *S. aureus* strains is the S84L mutation in the gyrA subunit. We tested compound **29** against a gyrase enzyme

DOI: 10.1021/acsinfecdis.7b00130
ACS Infect. Dis. 2018, 4, 158−174

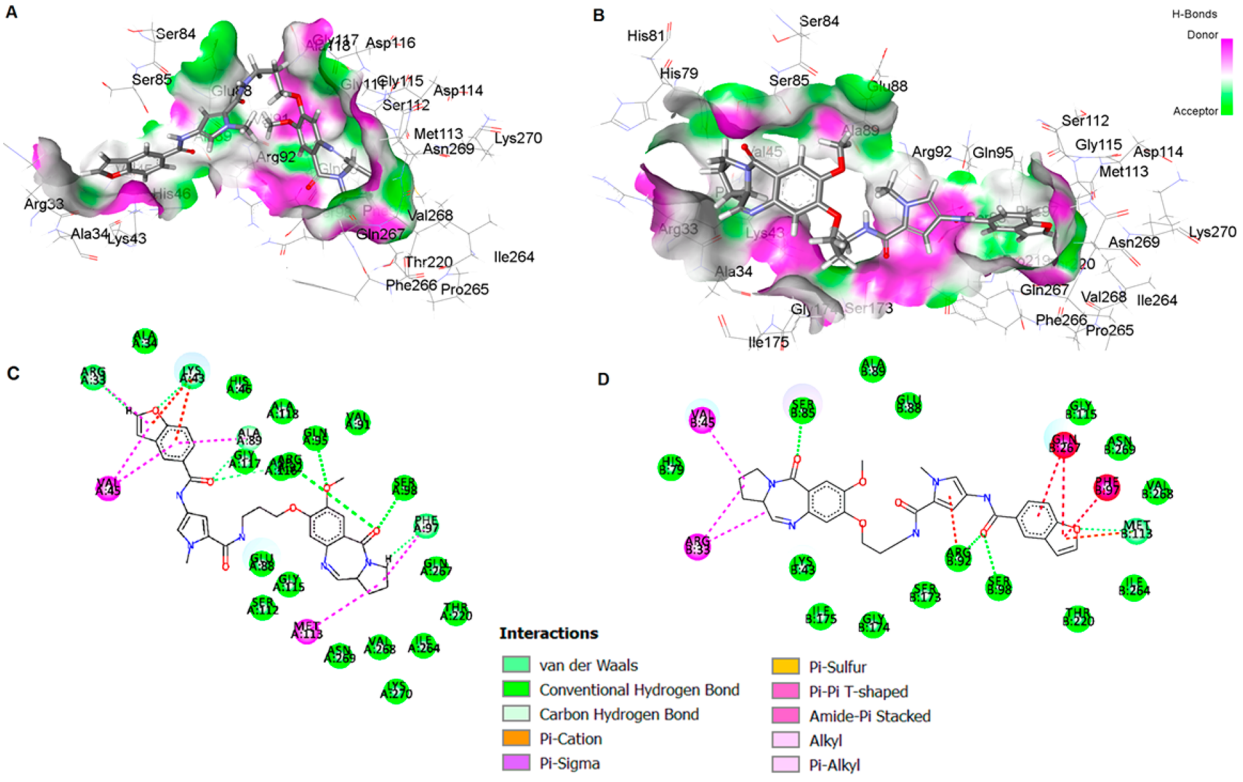

Figure 6. (A) Molecular model showing the interaction of compound **29** with the subunit 1 of the *S. aureus* gyrase A. (B) Molecular model showing the interaction of compound **29** with the subunit 2 of the *S. aureus* gyrase A. (C) 2D model showing the key interactions between compound **29** with the binding site in the subunit 1 of the *S. aureus* gyrase A. (D) 2D model showing the key interactions between compound **29** with the binding site in the subunit 2 of the *S. aureus* gyrase A.

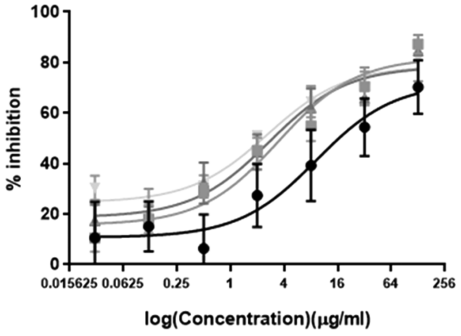

Figure 7. Biochemical analysis showing *S. aureus* gyrase enzyme inhibition by compounds **27** (■), **29** (▲), and **30** (▼) and ciprofloxacin (●) which was used as a control.

complex containing this mutation and found that, at 20 μg/mL, compound **29** inhibited the mutant enzyme by 60.0% ± 11.2%, while ciprofloxacin inhibited the mutant enzyme by just 43.3% ± 1.1% at the higher concentration of 32 μg/mL (Figure S9). This data suggests that compound **29** retains better activity against the fluoroquinolone-resistant enzyme than ciprofloxacin. The ability of compound **29** to inhibit the mutated DNA gyrase led us to carry out a further molecular modeling study to rationalize the biochemical assay result. The molecular model of gyrase A with S84L mutation in the gyrA subunit was developed with PyMol using PDB ID 2XCT as the template. The structure was minimized, equilibrated, and subsequently validated by the AMBER package program. Interestingly, compound **29** interacted with the ligand binding site of mutant gyrase A (Figure S2) with greater affinity and higher CHEMSCORE (23.4 for subunit 1 and 23.4 for subunit 2) compared to the wild-type enzyme. However, ciprofloxacin showed a significantly reduced affinity and CHEMSCORE (15.8 for subunit 1 and 15.9 for subunit 2) for the mutant enzyme (Figure S3, Table S3), which is consistent with the literature. Compound **29** formed five conventional hydrogen bonds with both subunit 1 and subunit 2 of the mutant enzyme (Tables S6 and S7). The antibacterial activity observed for compound **29** against *Staphylococcus* strains (Table 2) appeared to support the biochemical assay and the *in silico* observation as it showed similar activity (MIC 2−4 μg/mL) against the MSSA strain ATCC9144, which does not bear the S84L mutation in gyrase A and the MRSA strains, EMRSA-15 and EMRSA-16, with the S84L mutation in gyrase A.

■ CONCLUSIONS

This study was focused on understanding how the building blocks orientation of the lateral C8 side chain of PBDs affect the antibacterial activity of C8-PBD conjugates and the suitability of developing C8-linked inverted PBDs as antibacterial agents. Furthermore, we explored the suitability of using the novel 4C−NH_2 linker on the C8-position of the PBDs, which provides some advantages for the synthesis of the C8-linked pyrrolobenzodiazepines by avoiding the base catalyzed hydrolysis step that can result in C11a racemization. Four inverted C8-linked benzofused PBDs were successfully synthesized employing both 4C−COOH and 4C−NH_2 linkers. Two of them presented the inversion of the amide linkage between *N*-methylpyrrole and the PBD core while the other two presented the inversion of both amide bonds between the three moieties constituting the lateral chain and the

DOI: 10.1021/acsinfecdis.7b00130
ACS Infect. Dis. 2018, 4, 158−174

heterocyclic building blocks. The single amide bond inverted compounds showed notably inferior antibacterial activity owing to their inability to effectively associate with the DNA minor groove. However, the double inverted compounds showed comparable activity to the C8-benzofused PBDs with natural orientation. The inverted C8-analogues did not stabilize DNA sequences and showed selective toxicity toward prokaryotic cells. The differential sensitivity observed between *S. aureus* and *Enterococcus spp.* for compounds **31**, **32**, and to a lesser extent **28** is intriguing and pointed toward a new mechanism of action rather than solely DNA-binding, as observed for traditional DNA minor groove binders. *In silico* studies followed by biochemical assays suggested that the compounds are capable of binding to DNA gyrase and showed inhibition of DNA gyrase *in vitro*. The data in this study shows that these molecules can inhibit both wild-type and mutant DNA gyrase (S84L mutation in gyrase A) enzymes *in vitro* and kill *S. aureus* strains, carrying this mutation, that are resistant to fluoroquinolones. The observed IC_{50} is comparable to ciprofloxacin in the *in vitro* assay, and this was also the case for noninverted PBDs (**27** and **30**). Future studies are required to re-evaluate the mechanism of bacterial killing by this class of molecules, both in terms of the kinetics of the *in vitro* gyrase inhibition assay and by showing bacterial responses which are consistent with DNA-gyrase inhibition *in vivo*. This deeper understanding of the mechanism of action provides an opportunity to develop these inverted C8-PBD analogues as antibacterial agents due to their lack of eukaryotic toxicity and reasonable activity against MDR Gram-positive pathogens, potentially reviving PBD based anti-infective research.

METHODS

Chemistry. All solvents and reagents for the synthesis were obtained from commercially available sources, including, among others, Sigma-Aldrich, Fisher Scientific, Fluorochem, and Alfa Aesar. Thin-layer-chromatography (TLC) analysis was performed on silica gel plates (E. Merck silica gel 60 F254 plates) and visualized by ultraviolet (UV) radiation at 254 nm. Flash chromatography for the purification of compound was performed with silica gel as a stationary phase (Merck 60, 230−400 mesh). ^{1}H and ^{13}C nuclear magnetic resonance (NMR) analyses were performed on a Bruker Spectrosp in 400 Hz spectrometer. IR spectra were collected with an FT/IR IRAffinity-1S IR spectrophotometer (Shimadzu). HRMS was performed on a Thermo Scientific-Exactive HCD Orbitrap Mass Spectrometer. LC-MS analyses were performed on a Waters Alliance 2695 system, eluting in gradient with a flow rate of 0.5 mL/min using a solvent gradient starting with 5% acetonitrile that was increased to 95% acetonitrile over a 7.5 min time period (ESI). The analyses were performed on a Monolithic C18 50 × 4.60 mm column (made by Phenomenex). UV detection was performed on a diode array detector. Mass spectra were registered in both the ESI+ and ESI− mode. The hydrogenation reaction was conducted using a Parr hydrogenation system. A dynamic light scattering experiment was performed using a Nanoseries machine (Malvern Instruments, UK).

*Methyl 4-(4-Formyl-2-methoxyphenoxy)butanoate (**1**).* Methyl 4-bromobutanoate (17.7 mL, 140.2 mmol, 1.05 equiv) and potassium carbonate (30.4 g, 210.3 mmol, 1.5 equiv) were added to a solution of vanillin (20.0 g, 131.4 mmol, 0.9 equiv) in DMF (80 mL). The suspension was stirred at room temperature for 6 h, until TLC showed the completion of the reaction. At that point, H_2O (1 L) was added to the reaction, causing the formation of a precipitate that was filtered and collected giving pure **1** (32.0 g, 95%) as a white solid (melting point (mp) 65 °C).

R_f value (100% DCM): 0.62; ^{1}H NMR (400 MHz, $CDCl_3$) δ 9.84 (1H, s), 7.40−7.44 (2H, m), 6.98 (1H, d, J = 8 Hz), 4.16 (2H, t, J = 6.2 Hz), 3.92 (3H, s), 3.69 (3H, s), 2.56 (2H, t, J = 7.2 Hz), 2.17−2.23 (2H, m). ^{13}C NMR (100 MHz, $CDCl_3$) δ 190.9, 173.4, 153.8, 149.9, 130.3, 126.8, 111.5, 109.2, 67.8, 56.4, 51.7, 30.3, 24.2. m/z (+ESI) calc. for $C_{13}H_{16}O_5$ $(M)^+$ 252.2, found 253.1 $([M] + H)^+$.

*Methyl 4-(4-Formyl-2-methoxy-5-nitrophenoxy)-butanoate (**2**).* A solution of **1** (10.0 g, 39.6 mmol, 1.0 equiv) in trifluoroacetic acid (12 mL) was added dropwise to a solution of KNO_3 (5.0 g, 49.5 mmol, 1.25 equiv) in trifluoroacetic acid (12 mL) kept at 0 °C under a magnetic stirrer. After 40 min, TLC and LCMS monitoring showed completion of the reaction. The reaction mixture was evaporated under reduced pressure using a rotary evaporator. The residue was dissolved in EtOAc (50 mL), and the organic phase was washed with brine (3 × 50 mL). The organic phases were dried over $MgSO_4$ and concentrated by a rotary evaporator giving pure **2** (10.7 g, 92%) as an amber oil.

R_f value (100% DCM): 0.72; ^{1}H NMR (400 MHz, $CDCl_3$) δ 10.29 (1H, s), 7.46 (1H, s), 7.11 (1H, s), 4.06 (2H, t, J = 6.2 Hz), 3.85 (3H, s), 3.56 (3H, s), 2.42 (2H, t, J = 7.2 Hz), 2.04−2.11 (2H, m). ^{13}C NMR (100 MHz, $CDCl_3$) δ 188.5, 172.8, 152.7, 150.9, 143.5, 124.7, 110.5, 108.2, 67.8, 56.4, 51.3, 29.7, 23.2. m/z (+ESI) calc. for $C_{13}H_{15}NO_7$ $(M)^+$ 297.2, found 298.1 $([M] + H)^+$.

*5-Methoxy-4-(4-methoxy-4-oxobutoxy)-2-nitrobenzoic acid (**3**).* Compound **2** (10.0 g, 33.6 mmol, 1.0 equiv) was dissolved in acetone (400 mL). A hot solution of 10% potassium permanganate (275 mL) was added to the solution of **2** in a flask fitted with a condenser. The reaction mixture was left under reflux until the reaction went to completion (according to TLC). At that point, the reaction mixture was cooled down to room temperature. The brown residue formed was filtered through a Celite patch and washed with 600 mL of hot H_2O. A solution of 16% sodium bisulphite in 1 N HCl (400 mL) was added to the filtrate, and the pH of the solution was adjusted to 1 using concentrated HCl. This caused the precipitation of a yellow solid that was filtered, collected, and dried giving pure **3** (9.0 g, 82%) as a yellow solid (mp 114 °C).

R_f value (EtOAc/MeOH 50:50): 0.4; ^{1}H NMR (400 MHz, $CDCl_3$) δ 7.38 (1H, s), 7.21 (1H, s), 4.15 (2H, t, J = 5.8 Hz), 3.97 (3H, s), 3.70 (3H, s), 2.56 (2H, t, J = 7.2 Hz), 2.17−2.24 (2H, m). ^{13}C NMR (100 MHz, $CDCl_3$) δ 172.8, 166.0, 151.8, 149.1, 141.2, 121.3, 111.5, 107.2, 68.3, 56.4, 51.3, 29.7, 23.8. m/z (+ESI) calc. for $C_{13}H_{15}NO_8$ $(M)^+$ 313.2, found 312.1 $([M] - H)^-$.

*(S)-Methyl 4-(4-(2-(Hydroxymethyl)pyrrolidine-1-carbonyl)-2-methoxy-5-nitrophenoxy)butanoate (**4**).* A solution was prepared by dissolving **3** (7.9 g, 25.2 mmol, 1.0 equiv) in dry DCM (50 mL) in a round-bottom flask previously dried in an oven. Oxalyl chloride (6.5 mL, 75.6 mmol, 3 equiv) and a catalytic amount of DMF (2−3 drops) were added to the solution that initiated the reaction. The solution was left under a magnetic stirrer for 1 h until it ceased the formation of HCl. Dry toluene (15 mL) was added to the reaction mixture that was evaporated under reduced pressure in a rotary evaporator to eliminate the excess of oxalyl chloride. The reaction mixture was dissolved in dry DCM (50 mL), and the solution was

DOI: 10.1021/acsinfecdis.7b00130
ACS Infect. Dis. 2018, 4, 158−174

dropwise added to a solution of triethylamine (10.5 mL, 75.6 mmol, 3 equiv) and +(*S*)-pyrrolidinemethanol (3.7 mL, 37.8 mmol, 1.5 equiv) in dry DCM (30 mL) kept at 0 °C under N_2 atmosphere. The reaction mixture was then allowed to stir overnight. After 15 h, TLC showed the completion of the reaction, and the reaction mixture was extracted using 1 N HCl (2 × 70 mL) and brine (2 × 70 mL). The combined organic fractions were dried over $MgSO_4$ and concentrated by the rotary evaporator to give a yellow oil. The crude was purified by column chromatography (mobile phase: from EtOAc, 100, v/v, to EtOAc/MeOH, 98/2, v/v) affording pure **4** (5.5 g, 55%) as a pale yellow solid (mp 82 °C).

R_f value (EtOAc/MeOH 90:10): 0.46; ^{1}H NMR (400 MHz, $CDCl_3$) δ 7.69 (1H, s), 6.79 (1H, s), 4.14 (2H, t, J = 4.4 Hz), 3.96 (3H, s), 3.90 (1H, m), 3.78 (1H, m), 3.69 (3H, s), 3.16 (2H, t, J = 6.8 Hz), 2.55 (2H, t, J = 4.8 Hz), 2.10−2.22 (3 H, m), 1.70−1.90 (4 H, m). ^{13}C NMR (100 MHz, $CDCl_3$) δ 173.2, 154.8, 148.4, 109.2, 108.4, 68.4, 66.1, 61.5, 56.7, 51.7, 49.5, 30.3, 28.4, 24.4, 24.2. m/z (+ESI) calc. for $C_{18}H_{24}N_2O_8$ $(M)^+$ 396.3, found 397.0 $([M] + H)^+$.

*(S)-Methyl 4-(5-Amino-4-(2-(hydroxymethyl)pyrrolidine-1-carbonyl)-2-methoxyphenoxy)butanoate (**5**).* A catalytic amount of Pd/C (10% w/w) was added to a solution of **4** (5.5 g, 13 mmol, 1 equiv) in EtOH (100 mL). The reaction mixture was hydrogenated in a Parr hydrogenator at 40 psi for 4 h until TLC showed the completion of the reaction. At that point, the reaction was filtered under vacuum through a patch of Celite. The resulting solution was evaporated using a rotary evaporator giving pure **5** (4.5 g, 95%) as a dark yellow solid (mp 46 °C).

R_f value (EtOAc/MeOH 90:10): 0.36; ^{1}H NMR (400 MHz, $CDCl_3$) δ 6.76 (1H, s), 6.39 (1H, s), 4.39 (1H, bs), 4.03 (2H, t, J = 4.4 Hz), 3.78 (3H, s), 3.69 (3H, s), 3.62 (1H, m), 3.53 (1H, m), 2.54 (2H, t, J = 4.8 Hz), 2.15 (3H, m), 1.65−1.87 (4H, m). ^{13}C NMR (100 MHz, $CDCl_3$) δ 172.5, 170.7, 150.3, 140.5, 140.1, 135.0, 112.3, 110.5, 101.2, 66.5, 59.9, 56.3, 52.4, 50.6, 29.4, 27.5, 23.9, 23.4. m/z (+ESI) calc. for $C_{18}H_{26}N_2O_6$ $(M)^+$ 366.4, found 367.2 $([M] + H)^+$.

*(S)-Methyl 4-(5-(Allyloxycarbonylamino)-4-(2-(hydroxymethyl)pyrrolidine-1-carbonyl)-2-methoxyphenoxy)butanoate (**6**).* A solution was prepared by dissolving **5** (3.3 g, 9 mmol, 1.0 equiv) in dry DCM (40 mL). Dry pyridine (1.7 mL, 21.1 mmol, 2.3 equiv) and a solution of allyl chloroformate (0.91 mL, 8.5 mmol, 0.95 equiv) in anhydrous DCM (30 mL) were sequentially added to this solution, which was kept at −10 °C under N_2 atmosphere. The reaction mixture was left under a magnetic stirrer at room temperature for 2 h, until TLC showed the completion of the reaction. At that point, the reaction mixture was extracted with a saturated $CuSO_4$ solution (70 mL), saturated aqueous $NaHCO_3$ (100 mL), and brine (100 mL). The organic phase was dried over $MgSO_4$ and concentrated under reduced pressure using a rotary evaporator. The crude of the reaction was subsequently purified by column chromatography (mobile phase: EtOAc, 100%) affording pure **6** (3.6 g, 88%) as a pale yellow solid (mp 49 °C)

R_f value (DCM/acetone 60:40): 0.51; ^{1}H NMR (400 MHz, $CDCl_3$) δ 8.72 (1H, bs), 7.77 (1H, s), 6.82 (1H, s), 5.95 (1H, m), 5.35 (1H, dd, J = 17.2, 1.2 Hz), 5.23 (1H, dd, J = 10.0, 0.8 Hz), 4.63 (2H, dd, J = 5.6, 1.2 Hz), 4.40 (1H, bs), 4.11 (2H, t, J = 4.4 Hz), 3.82 (3H, s), 3.61 (3H, s), 3.59 (1H, m), 3.50 (1H, m), 2.54 (2H, t, J = 4.8 Hz), 2.17 (3H, m), 1.72−1.92 (4H, m). ^{13}C NMR (100 MHz, $CDCl_3$) δ 173.4, 170.9, 153.6, 150.5, 144.0, 132.3, 131.9, 118.2, 115.7, 111.6, 105.6, 67.7, 66.6, 65.7, 61.6, 60.4, 56.6, 51.7, 30.7, 28.3, 25.1, 24.3. m/z (+ESI) calc. for $C_{22}H_{30}N_2O_8$ $(M)^+$ 450.4, found 451.2 $([M] + H)^+$.

*Allyl 11-Hydroxy-7-methoxy-8-(4-methoxy-4-oxobutoxy)-5-oxo-2,3,11,11a-hexahydro-1H-pyrrolo[2,1-c][1,4]-benzodiazepine-10(5H)-carboxylate (**7**).* BAIB (3.7 g, 11.6 mmol, 1.2 equiv) and TEMPO (152.0 mg, 1.0 mmol, 0.1 equiv) were sequentially added to a solution of **6** (4.41 g, 9.7 mmol, 1.0 equiv) in DCM (200 mL). The reaction was left under a magnetic stirrer for 6 h until TLC showed the completion of the reaction. At that point, the reaction mixture was sequentially washed with saturated sodium metabisulphite (100 mL), saturated aqueous $NaHCO_3$ (2 × 100 mL), and brine (100 mL). The organic phase was dried over $MgSO_4$ and concentrated under reduced pressure using a rotary evaporator. The crude of the reaction was purified by column chromatography (mobile phase: EtOAc/hexane, 50/50, v/v) affording pure **7** (3.3 g, 75%) as a yellow solid (mp 74 °C).

R_f value (DCM/acetone 60:40): 0.51; ^{1}H NMR (400 MHz, $CDCl_3$) δ 7.22 (1H, s), 6.69 (1H, s), 5.80 (1H, m), 5.62 (1H, d, J = 4.0 Hz), 5.07 (2H, d, J = 12.0 Hz), 4.61 (1H, dd, J = 13.2, 5.6 Hz), 4.41 (1H, bs), 4.21 (2H, d, J = 12.0 Hz), 3.89 (3H, s), 3.67 (3H, s), 3.49 (1H, t, J = 8.0 Hz), 3.43 (1H, m), 2.48 (2H, t, J = 7.2 Hz), 2.12 (4H, m), 1.95 (2H, m). ^{13}C NMR (100 MHz, $CDCl_3$) δ 173.4, 167.0, 155.9, 149.9, 148.7, 131.8, 128.3, 126.0, 117.9, 114.2, 110.8, 85.9, 67.9, 66.7, 60.3, 60.1, 56.1, 51.6, 46.3, 30.3, 28.7, 24.2, 23.0, 20.9. m/z (+ESI) calc. for $C_{22}H_{28}N_2O_8$ $(M)^+$ 448.4, found 449.2 $([M] + H)^+$.

*Allyl 7-Methoxy-8-(4-methoxy-4-oxobutoxy)-5-oxo-11-(tetrahydro-2H-pyran-2-yloxy)-2,3,11,11a-hexahydro-1H-pyrrolo[2,1-c][1,4]benzodiazepine-10(5H)-carboxylate (**8**).* DHP (6.3 mL, 75.0 mmol, 10.0 equiv) was added to a solution of **7** (3.3 g, 7.5 mmol, 1.0 equiv) in the presence of a catalytic amount of PTSA (33.0 mg, 0.2 mmol, 0.03 equiv) in EtOAc (50 mL). The reaction mixture was left under a magnetic stirrer for 2 h until TLC showed the completion of the reaction. At that point, the reaction mixture was extracted with saturated aqueous $NaHCO_3$ (2 × 50 mL) and brine (50 mL). The organic phase was dried over $MgSO_4$ and evaporated using a rotary evaporator under reduced pressure. The crude of the reaction was purified by column chromatography (mobile phase: DCM/acetone, 90/10, v/v) affording pure **8** (3.6 g, 85%) as a yellow solid (mp 53 °C).

R_f value (DCM/acetone 60:40): 0.67; ^{1}H NMR (400 MHz, $CDCl_3$) δ 7.19 (1 H, s), 6.88 (1 H, s), 6.60 (1 H, s), 5.68−5.90 (4 H, m), 5.00−5.20 (8 H, m), 4.30−4.70 (4 H, m), 4.05−4.15 (6 H, m), 3.80−3.92 (8 H, m), 3.62−3.73 (8 H, m), 3.40- 3.55 (8 H, m), 2.50−2.64 (4 H, m), 2.90−2.10 (8H, m), 1.65−1.84 (6 H, m), 1.42−1.62 (15 H, m). ^{13}C NMR (100 MHz, $CDCl_3$) δ 173.4, 167.4, 149.1, 132.0, 114.9, 100.0, 98.4, 96.1, 94.6, 91.7, 88.6, 68.0, 67.7, 66.5, 63.6, 62.9, 60.1, 56.1, 51.6, 51.2, 46.3, 30.9, 30.2, 29.0, 25.4, 24.2, 20.0. m/z (+ESI) calc. for $C_{27}H_{36}N_2O_9$ $(M)^+$ 532.5, found 533.2 $([M] + H)^+$.

*4-(10-(Allyloxycarbonyl)-7-methoxy-5-oxo-11-(tetrahydro-2H-pyran-2-yloxy)-2,3,5,10,11,11a-hexahydro-1H-pyrrolo[2,1-c][1,4]benzodiazepine-8-yloxy)butanoic acid (**9**).* An excess of NaOH 1 M aqueous solution was added to a solution of **8** (3.8 g, 7.1 mmol, 1.0 equiv) in MeOH (60 mL). The reaction mixture was left under a magnetic stirrer overnight until TLC showed the completion of the reaction. MeOH was evaporated under reduced pressure using a rotary evaporator, and H_2O (30 mL) was added to the residue. Citric acid (1 M aqueous solution) was added until acidic pH was

DOI: 10.1021/acsinfecdis.7b00130
ACS Infect. Dis. 2018, 4, 158−174

reached. The aqueous layer was then extracted with EtOAc (2 × 50 mL). The combined organic layers were dried over $MgSO_4$ and concentrated under reduced pressure using a rotary evaporator, giving pure PBD protected acid core **9** (3.2 g, 87%) as a light yellow solid (mp 72 °C).

R_f value (DCM/acetone 60:40): 0.27; ^{1}H NMR (400 MHz, $CDCl_3$) δ 7.20 (2 H, s), 6.89 (1 H, s), 6.58 (1 H, s), 5.87 (2 H, d, J = 9.2 Hz), 5.72 (2 H, d, J = 9.2 Hz), 4.95−5.18 (5 H, m), 4.30−4.60 (5 H, m), 4.00−4.15 (7 H, m), 3.82−3.91 (7 H, m), 3.42−3.69 (9 H, m), 2.49−2.60 (4 H, m), 1.90−2.20 (12 H, m), 1.67−1.81 (4 H, m), 1.40−1.60 (8 H, m). ^{13}C NMR (100 MHz, $CDCl_3$) δ 177.6, 167.6, 149.8, 132.1, 131.9, 126.7, 117.3, 114.9, 110.8, 100.7, 96.0, 91.7, 88.5, 67.9, 66.6, 63.6, 60.1, 56.1, 46.5, 31.1, 30.3, 28.8, 25.2, 24.1, 23.2, 20.0. m/z (+ESI) calc. for $C_{26}H_{34}N_2O_9$ $(M)^+$ 518.5, found 519.2 $([M] + H)^+$.

*4-(Benzyloxy)-3-methoxybenzaldehyde (**10**).* Benzyl bromide (12.9 mL, 108.4 mmol, 1.1 equiv) and potassium carbonate (6.8 g, 49.3 mmol, 0.5 equiv) were added to a solution of vanillin (15.0 g, 98.6 mmol, 1.0 equiv) in acetone (225 mL). The suspension was stirred under reflux overnight until TLC showed the completion of the reaction. At that point, H_2O (5000 mL) was added to the reaction, causing the formation of a precipitate that was filtered and recrystallized from EtOH at 0 °C giving pure **10** (14.9 g, 62%) as a pale yellow solid (mp 61 °C).

R_f value (100% DCM): 0.71; ^{1}H NMR (400 MHz, $CDCl_3$) δ 9.83 (1H, s), 7.29−7.46 (7H, m), 6.98 (1H, d, J = 8.06 Hz), 5.25 (2H, s), 3.94 (3H, s). ^{13}C NMR (100 MHz, $CDCl_3$) δ 191.0, 153.6, 150.1, 136.0, 130.3, 128.7, 128.2, 127.2, 126.6, 112.3, 109.3, 70.9, 56.1. m/z (+ESI) calc. for $C_{15}H_{14}O_3$ $(M)^+$ 242.3, found 242.9 $([M] + H)^+$.

*4-(Benzyloxy)-5-methoxy-2-nitrobenzaldehyde (**11**).* A solution of **10** (14.8 g, 61.1 mmol, 1.0 equiv) in trifluoroacetic acid (18 mL) was added dropwise to a solution of KNO_3 (7.7 g, 76.4 mmol, 1.25 equiv) in trifluoroacetic acid (18 mL) kept at 0 °C under a magnetic stirrer. After 40 min, the reaction went to completion by TLC and LCMS. The reaction mixture was evaporated under reduced pressure using a rotary evaporator. The residue was dissolved in EtOAc (500 mL), and the organic phase was washed with brine (3 × 500 mL). The organic phases were dried over $MgSO_4$ and concentrated by a rotary evaporator giving pure **11** (14.5 g, 98%) as a bright yellow solid (mp 114 °C).

R_f value (100% DCM): 0.73; ^{1}H NMR (400 MHz, $CDCl_3$) δ 10.42 (1H, s), 7.66 (1H, s), 7.34−7.46 (6H, m), 5.26 (2H, s), 4.0 (3H, s). ^{13}C NMR (100 MHz, $CDCl_3$) δ 187.8, 153.7, 151.4, 134.85, 129.0, 128.9, 128.7, 127.6, 125.7, 110.0, 108.9, 71.6, 56.7. m/z (+ESI) calc. for $C_{15}H_{13}NO_5$ $(M)^+$ 287.3, found 285.9 $([M] - H)^-$.

*4-Hydroxy-5-methoxy-2-nitrobenzaldehyde (**12**).* A solution of **11** (14.4 g, 50.1 mmol, 1 equiv) in acetic acid (120 mL) was heated up to 85 °C, and a hydrobromic acid solution (48%, 40 mL) was added. The mixture was kept under a magnetic stirrer for 1 h. The solid product obtained was filtered and recrystallized from hot EtOH. The solid obtained was dried in a vacuum oven giving pure **12** (6.1 g 62%) as a yellow solid (mp 212 °C).

R_f value (100% DCM): 0.51; ^{1}H NMR (400 MHz, DMSO-*d*) δ 11.12 (1H, br s), 10.16 (1H, s), 7.50 (1H, s), 7.35 (1H, s), 3.94 (3H, s). ^{13}C NMR (100 MHz, DMSO-*d*) δ 188.3, 151.8, 151.0, 143.7, 123.4, 111.0, 110.6, 56.31. m/z (+ESI) calc. $C_8H_7NO_5$ $(M)^+$ 197.2, found 198.0 $([M] + H)^+$.

*tert-Butyl (3-(4-Formyl-2-methoxy-5-nitrophenoxy)-propyl)carbamate (**13**).* *tert*-Butyl (3-bromopropyl)carbamate (7.1 g, 29.6 mmol, 1.05 equiv) and potassium carbonate (5.8 g, 42.3 mmol, 1.5 equiv) were added to a solution of **12** (5.6 g, 28.2 mmol, 1.0 equiv) in DMF (22 mL). The suspension was stirred at 50 °C for 24 h, until TLC showed the completion of the reaction. At that point, H_2O (500 mL) was added to the reaction, and the product was extracted in EtOAc. The organic solvent was then evaporated using the rotary evaporator, and the compound was purified by flash column chromatography (mobile phase hexane/EtOAc, 80:20, v/v) to give pure **13** (9.3 g, 93%) as a brown oil.

R_f value (100% DCM): 0.68; ^{1}H NMR (400 MHz, $CDCl_3$) δ 10.44 (1H, s), 7.59 (1H, s), 7.41 (1H, s), 4.23 (2H, t, J = 5.92), 4.01 (3H, s), 3.34−3.43 (2H, m), 2.05−2.13 (2H, m), 1.45 (9H, s). ^{13}C NMR (100 MHz, $CDCl_3$) δ 188.5, 155.6, 152.6, 151.2, 143.5, 124.6, 110.0, 108.1, 77.6, 67.3, 56.4, 35.7, 28.8, 28.1. m/z (+ESI) calc. $C_{16}H_{22}N_2O_7$ $(M)^+$ 354.4, found 255.0 $([M] + H\text{-Boc})^+$, 377.0 $([M] + Na)^+$.

*4-(3-((tert-Butoxycarbonyl)amino)propoxy)-5-methoxy-2-nitrobenzoic acid (**14**).* Compound **13** (9.2 g, 25.9 mmol, 1.0 equiv) was dissolved in acetone (500 mL). A hot solution of 10% potassium permanganate (250 mL) was added to the solution of **13** in a flask fitted with a condenser. The reaction mixture was left under reflux until the reaction went to completion (according to TLC). At that point, the reaction mixture was cooled down to room temperature. The brown residue formed was filtered through a Celite path and washed with 600 mL of hot H_2O. A solution of sodium bisulphite (16%, 400 mL) was added to the filtrate, and the pH of the solution was adjusted to 3.5 using concentrated citric acid. The product was then extracted in EtOAc. The organic solvent was removed using the rotary evaporator, giving **14** (8.1 g, 83%) as a yellow solid (mp 107 °C).

R_f value (EtOAc/MeOH 50:50): 0.57; ^{1}H NMR (400 MHz, $CDCl_3$) δ 7.29 (1H, s), 7.08 (1H, br s), 4.10 (2H, t, J = 5.29 Hz), 3.89 (3H, s), 3.31−3.38 (2H, m), 2.02 (2H, quin, J = 5.79 Hz), 1.44 (9H, s). ^{13}C NMR (100 MHz, $CDCl_3$) δ 191.1, 156.2, 152.7, 149.0, 128.7, 127.2, 110.8, 107.6, 79.3, 68.3, 56.5, 38.4, 28.5, 28.4. m/z (+ESI) calc. $C_{16}H_{22}N_2O_8$ $(M)^+$ 370.4, found 271.0 $([M] + H\text{-Boc})^+$, 393.1 $([M] + Na)^+$.

*tert-Butyl (S)-(3-(4-(2-(Hydroxymethyl)pyrrolidine-carbonyl)-2-methoxy-5-nitrophenoxy)propyl)carbamate (**15**).* A solution was prepared by dissolving **14** (8.0 g, 21.6 mmol, 1.1 equiv), HBTU (18.6 g, 49.0 mmol, 2.5 equiv), and DIPEA (10.2 mL, 58.8 mmol, 3 equiv) in DMF (250 mL). The solution was left under a magnetic stirrer for 20 min. Then, (*S*)-(+)-2-pyrrolidinemethanol (1.93 mL, 19.6 mmol, 1.0 equiv) was added to the mixture which was kept under magnetic stirring at 50 °C for 15 h until TLC showed the completion of the reaction. At that point, water was added to the reaction mixture, and the product was extracted in EtOAc. The organic phase was then washed with brine and a saturated $NaHCO_3$ solution. The organic solution was concentrated using a rotary evaporator, and the product was purified by flash column chromatography (mobile phase: from 100% EtOAc to EtOAc/MeOH, 98:2, v/v) to afford pure **15** (3.2 g, 35%) as brown solid (mp 68 °C).

R_f value (EtOAc/MeOH 90:10): 0.42; ^{1}H NMR (400 MHz, $CDCl_3$) δ 7.67 (1H, s), 6.79 (1H, s), 4.16 (2H, t, J = 5.92 Hz), 3.97 (3H, s), 3.85−3.91 (1H, m), 3.75−3.82 (1H, m), 3.33−3.40 (2H, m), 3.15 (2H, t, J = 6.55), 2.12−2.21 (2H, m), 2.03−2.09 (2H, m), 1.68−1.93(4H, m), 1.44 (9H, s). ^{13}C NMR (100

DOI: 10.1021/acsinfecdis.7b00130
ACS Infect. Dis. 2018, 4, 158−174

MHz, $CDCl_3$) δ 200.7, 156.0, 154.7, 153.2, 148.3, 127.9, 109.0, 108.0, 79.2, 68.4, 61.6, 56.7, 49.5, 38.5, 29.1, 28.5, 24.4. *m/z* (+ESI) calc. $C_{21}H_{31}N_3O_8$ $(M)^+$ 453.5, found 454.1 $([M] + H)^+$.

*tert-Butyl (S)-(3-(5-Amino-4-(2-(hydroxymethyl)-pyrrolidine-1-carbonyl)-2-methoxyphenoxy)propyl)-carbamate (**16**).* A catalytic amount of Pd/C (10% w/w) was added to a solution of **15** (3.2 g, 7.1 mmol, 1.0 equiv) in EtOH (30 mL). The reaction mixture was hydrogenated in a Parr hydrogenator at 40 psi overnight until TLC showed the completion of the reaction. At that point, the reaction was filtered under vacuum through a path of Celite. The resulting solution was evaporated using a rotary evaporator giving pure **16** (2.9 g, 96%) as a yellow solid (mp 73 °C).

R_f value (EtOAc/MeOH 90:10): 0.65; ^{1}H NMR (400 MHz, $CDCl_3$) δ 6.72 (1H, s), 6.23 (1H, s), 4.04 (2H, t, *J* = 5.79 Hz), 3.79 (3H, s), 3.57−3.71 (2H, m), 3.51 (2H, td, *J* = 10.13, 6.42 Hz), 3.30−3.39 (2H, m), 2.10−2.20 (1H, m), 2.00 (2H, quin, *J* = 5.85 Hz), 1.58−1.93 (4H, m), 1.45 (9H, s). ^{13}C NMR (100 MHz, $(CD_3)_2SO$) δ 170.3, 168.5, 155.6, 150.1, 140.0, 112.9, 101.6, 101.2, 77.5, 65.8, 61.4, 61.4, 58.5, 56.4, 37.2, 29.1, 28.2, 27.1, 20.7. *m/z* (+ESI) calc. $C_{21}H_{33}N_3O_6$ $(M)^+$ 423.5, found 424.1 ([M] + H).

*tert-Butyl (S)-(3-(5-(((Allyloxy)carbonyl)amino)-4-(2-(hydroxymethyl)pyrrolidine-1-carbonyl)-2-methoxyphenoxy)propyl)carbamate (**17**).* A solution was prepared by dissolving **16** (2.8 g, 6.6 mmol, 1.0 equiv) in dry DCM (82 mL). Dry pyridine (1.42 mL) and a solution of allyl chloroformate (0.67 mL, 6.3 mmol, 0.95 equiv) in anhydrous DCM (57.38 mL) were sequentially added to this solution, which was kept at −10 °C under an N_2 atmosphere. The reaction mixture was left under a magnetic stirrer at room temperature for 2 h, until TLC showed the completion of the reaction. At that point, the reaction mixture was extracted with a saturated $CuSO_4$ solution (100 mL), saturated aqueous $NaHCO_3$ (200 mL), and brine (200 mL). The organic phase was dried over $MgSO_4$ and concentrated under reduced pressure using a rotary evaporator. Pure **17** (3.1 g, 94%) was obtained as a brown solid (mp 47 °C).

R_f value (EtOAc/MeOH 90:10): 0.54; ^{1}H NMR (400 MHz, $CDCl_3$) δ 7.73 (1H, dr s), 6.80 (1H, s), 5.87−6.01 (1H, m), 5.34 (1H, dd, *J* = 17.37,1.51 Hz), 5.23 (1H, dd, *J* = 10.32, 1.26 Hz), 4.62 (2H, dq, *J* = 5.70, 1.46 Hz), 4.13 (2H, t, *J* = 5.67 Hz), 3.83 (3H, s), 3.39−3.75 (4H, m), 3.34 (2H, q, *J* = 5.71), 2.10−2.20 (1H, m), 2.01 (2H, quin, *J* = 5.85 HZ), 1.86−1.91 (2H, m), 1.60−1.79 (2H, m), 1.44 (9H, s). ^{13}C NMR (100 MHz, $CDCl_3$) δ 170.9, 156.1, 153.7, 150.3, 144.0, 132.5, 131.8, 118.2, 110.9, 105.4, 78.9, 68.0, 66.5, 65.8, 61.1, 56.3, 51.6, 38.8, 29.1, 28.5, 28.3, 25.15. *m/z* (+ESI) calc. $C_{25}H_{37}N_3O_8$ $(M)^+$ 507.6, found 508.2 $([M] + H)^+$.

*Allyl-8(3-((tert-butoycarbonyl)amino)propoxy)-11-hydroxy-7-methoxy-5-oxo-2,3,11,11a-tetrahydro-1H-benzo[e]-pyrrolo[1,2-α][1,4]diazepine-10-(5H)carboxylate (**18**).* BAIB (2.4 g, 7.4 mmol, 1.2 equiv) and TEMPO (0.1 g, 0.6 mmol, 0.1 equiv) were sequentially added to a solution of **17** (3.14 g, 6.2 mmol, 1 equiv) in DCM (160 mL). The reaction was stirred for 6 h until TLC showed the completion of the reaction. At that point, the reaction mixture was sequentially washed with saturated sodium metabisulphite (100 mL), saturated aqueous $NaHCO_3$ (2 × 100 mL), and brine (100 mL). The organic phase was dried over $MgSO_4$ and concentrated under reduced pressure using a rotary evaporator. The crude of the reaction was purified by column chromatography (mobile phase: EtOAc/DCM, 50/50, v/v) affording pure **18** (3 g, 96%) as an ochre solid (mp 75 °C).

R_f value (EtOAc/MeOH 90:10): 0.48; ^{1}H NMR (400 MHz, $CDCl_3$) δ 7.22 (1H, s), 6.65 (1H, s), 5.69−5.84 (1H, m), 5.57−5.65 (1H, m), 5.46 (1H, br s), 4.64 (1H, dd, *J* = 13.35, 5.04 Hz), 4.42 (1H, dd, 13.35, 4.28 Hz), 4.01−4.07 (2H, m), 3.90 (3H, s), 3.64−3.71 (1H, m), 3.41−3.57 (2H, m), 3.32 (2H, d, *J* = 5,29 Hz), 2.06−2.13 (2H, m), 1.87−2.02 (5H,m), 1.43 (9H, s). ^{13}C NMR (100 MHz, $CDCl_3$) δ 166.9, 156.1, 155.9, 149.8, 148.6, 131.8, 128.4, 126.1, 118.0, 113.7, 110.5, 86.0, 79.0, 68.2, 66.7, 60.0, 56.0, 53.5, 46.4, 38.8, 29.1, 28.7, 28.5, 23.0. *m/z* (+ESI) calc. $C_{25}H_{35}N_3O_8$ $(M)^+$ 505.6, found 506.2 $([M] + H)^+$.

*General Procedure Adopted for Amide Coupling Reactions of the Biaryl Moieties (**19**−**24**).* DMAP (3 equiv) and EDCI (2 equiv) were added to a solution of carboxylic acid in DMF (6 mL). The mixture was kept under N_2 atmosphere and magnetic stirring for 30 min. Subsequently, the amino compound (1.5 equiv) was added to the solution, which was left under a magnetic stirrer at room temperature overnight. An aqueous solution of citric acid at pH = 2.5 (40 mL) was added to the mixture, and the product was extracted with EtOAc. The organic phase was washed with brine and concentrated using a rotary evaporator. The crude product was purified by flash column chromatography (mobile phase: from DCM, 100%, to DCM/acetone, 70/30, v/v.

*tert-Butyl (5-(Benzofuran-5-ylcarbamoyl)-1methyl-1H-pyrrol-3-yl)carbamate (**19**).* The reaction afforded 330.0 mg (67%) as pale brown solid (mp 176 °C).

R_f value (DCM/acetone 80:20): 0.71; ^{1}H NMR (400 MHz, $CDCl_3$) δ 7.89 (1H, d, *J* = 1.51 Hz), 7.81 (1H, br s), 7.58 (1H, d, *J* = 2.27 Hz), 7.39 (1H, d, *J* = 8.56 Hz), 7.24 (1H, d, *J* = 8.5 6 Hz), 6.83 (1H, s), 6.68 (1H, dd, *J* = 2.14, 0.88 Hz), 6.63 (1H, s), 6.47 (1H, s), 3.85 (3H, s), 1.49 (9H, s). ^{13}C NMR (100 MHz, $CDCl_3$) δ 160.0, 153.6, 151.8, 145.8, 133.0, 127.8, 123.5, 121.8, 118.7, 117.9, 113.2, 111.4, 106.8, 103.9, 80.3, 36.7, 28.4. *m/z* (+ESI) calc. for $C_{19}H_{21}N_3O_4$ $(M)^+$ 355.4, found 355.8 $([M] + H)^+$.

*N-(Benzofuran-5-yl)-4-cyano-1-methyl-1H-pyrrole-2-carboxamide (**20**).* The reaction afforded 429.0 mg (79%) as yellow solid (mp 172 °C).

R_f value (DCM/acetone 80:20): 0.69; ^{1}H NMR (400 MHz, $CDCl_3$) δ 7.92 (1H, d, *J* = 2.27 Hz), 7.80 (1H, s), 7.64 (1H, d, *J* = 2.01 Hz), 7.48 (1H, d, *J* = 8.81), 7.31 (1H, dd, *J* = 8.69, 2.14 Hz), 7.24 (1H, d, *J* = 1.76 Hz), 6.99 (1H, d, *J* = 1.51 Hz), 6.76 (1H, dd, *J* = 2.27, 1.01 Hz), 4.01 (3H, s). ^{13}C NMR (100 MHz, $CDCl_3$) δ 158.6, 152.2, 146.1, 133.6, 132.3, 128.0, 127.5, 118.0, 115.6, 114.7, 113.5, 111,7, 106.8, 92.1, 37.7. *m/z* (+ESI) calc. for $C_{15}H_{11}N_3O_2$ $(M)^-$ 265.3, found 263.9 $([M] - H)^-$.

*Methyl 4-(Benzofuran-5-carboxamido)-1-methyl-1H-pyrrole-2-carboxylate (**21**).* The reaction afforded 144.0 mg (20%) as dark yellow solid (mp 163 °C).

R_f value (DCM/acetone 80:20): 0.63; ^{1}H NMR (400 MHz, $CDCl_3$) δ 8.12 (1H, d, *J* = 1.51 Hz), 7.89 (1H, s), 7.79 (1H, dd, *J* = 8.69, 1.64 Hz), 7.70 (1H, d, *J* = 2.27 Hz), 7.55 (2H, dd, *J* = 4.91, 3.15 Hz), 6.83 (1H, d, *J* = 2.27 Hz), 6.80 (1H, d, *J* = 1.76 Hz), 3.91 (3H, s), 3.81 (3H, s). ^{13}C NMR (100 MHz, $CDCl_3$) δ 165.0, 161.5, 156.6, 146.4, 129.5, 127.7, 123.4, 121.9, 121.4, 120.7, 119.8, 111.6, 108.2, 107.0, 51.2, 36.9. *m/z* (+ESI) calc. for $C_{16}H_{14}N_2O_4$ $(M)^+$ 298.3, found 299.1 $([M] + H)^+$.

*tert-Butyl (5-(Benzo[b]thiophene-5-ylcarbamoyl)-1-methyl-1H-pyrrol-3-yl)carbamate (**22**).* The reaction afforded 435.0 mg (93%) as brown solid (mp 164 °C).

DOI: 10.1021/acsinfecdis.7b00130
ACS Infect. Dis. 2018, 4, 158−174

R_f value (DCM/acetone 80:20): 0.7; ^{1}H NMR (400 MHz, $CDCl_3$) δ 8.21 (1H, d, J = 2.01 Hz), 7.80 (1H, d, J = 8.81), 7.70 (1H, s), 7.45 (1H, d, J = 5.29 Hz), 7.35 (1H, dd, J = 8.81, 2.01 Hz), 7.29 (1H, d, J = 5.54 Hz), 6.86 (1H, s), 6.67 (1H, s), 6.29 (1H, br s), 3.92 (3H, s), 1.51 (9H, s). ^{13}C NMR (100 MHz, $CDCl_3$) δ 159.7, 153.5, 140.3, 135.3, 134.7, 127.5, 124.0, 123.5, 122.7, 121.8, 118.7, 117.7, 114.6, 103.8, 80.4, 36.8, 28.4. m/z (+ESI) calc. for $C_{19}H_{21}N_3O_3S$ $(M)^+$ 371.5, found 372.0 $([M] + H)^+$.

*N-(Benzo[b]thiophene-5-yl)-4-cyano-1-methyl-1H-pyrrole-2-carboxamide (**23**).* The reaction afforded 970.3 mg (92%) as brown solid (mp 173 °C).

R_f value (DCM/acetone 80:20): 0.66; ^{1}H NMR (400 MHz, $CDCl_3$) δ 8.20 (1H, d, J = 2.01 Hz), 7.39 (1H, br s), 7.83 (1H, d, J = 8.56 Hz), 7.48 (1H, d, J = 5.54 Hz), 7.39 (1H, dd, J = 8.69, 2.14 Hz), 7.30 (1H, d, J = 5.29 Hz), 7.24 (1H, d, J = 1.74 Hz), 7.02 (1H, d, J = 1.51 Hz), 4.01 (3H, s). ^{13}C NMR (100 MHz, $CDCl_3$) δ 158.6, 140.2, 136.0, 134.1, 133.7, 127.8, 127.4, 123.9, 122.9, 117.9, 115.5, 115.1, 114.8, 92.1, 37.7. m/z (+ESI) calc. for $C_{15}H_{11}N_3OS$ $(M)^-$ 281.3, found 281.9 $([M] + H)^+$.

*Methyl (4-Benzo[b]thiophene-5-carboxamido)-1-methyl-1H-pyrrole-2-carboxylate (**24**).* The reaction afforded 390.0 mg (88%) as white solid (mp 214 °C).

R_f value (DCM/acetone 80:20): 0.65; ^{1}H NMR (400 MHz, $CDCl_3$) δ 8.28−8.30 (2H, m), 7.84−7.89 (1H, m), 7.77 (1H, dd, J = 8.56, 1.76 Hz), 7.52 (1H, d, J = 2.01 Hz), 7.49 (1H, d, J = 5.54 Hz), 7.32 (1H, d, J = 5.29 Hz), 6.83 (1H, d, J = 2.01 Hz), 3.86 (3H, s), 3.78 (3H, s). ^{13}C NMR (100 MHz, $CDCl_3$) δ 165.0, 161.5, 142.8, 139.5, 130.6, 128.0, 124.2, 122.7, 122.6, 122.34, 121.9, 121.4, 119.9, 108.4, 51.2, 36.9. m/z (+ESI) calc. for $C_{16}H_{14}N_2O_3S$ $(M)^+$ 314.4, found 314.9 $([M] + H)^+$.

*General Procedure Adopted for the Nitrile Hydrolysis (**25**, **26**).* The biaryl compound bearing the nitrile group was solubilized in a mixture of dioxane (4 mL) and water (10 mL), and concentrated H_2SO_4 (2 mL) was added to this mixture. The solution was kept under magnetic stirring at 80 °C for 96 h. A saturated solution of $NaHCO_3$ was slowly added until the mixture reached pH = 8, and then, it was washed with EtOAc (250 mL). The concentrated HCl was added to the aqueous phase to reach pH = 2, and the product was extracted with EtOAc (300 mL). The organic phase was concentrated using a rotary evaporator, and the crude product was purified by flash column chromatography (mobile phase: from 100% EtOAc to EtOAc/MeOH, 95/5, v/v).

*5-(Benzofuran-5-ylcarbamoyl)-1-methyl-1H-pyrrole-3-carboxylic acid (**25**).* The reaction afforded 39.0 mg (9%) as brown solid (186 °C).

R_f value (acetone/DCM 80:20): 0.37; ^{1}H NMR (400 MHz, $(CD_3)_2SO$) δ 10.03 (1H, s), 8.09 (1H, d, J = 1.51 Hz), 7.69 (1H, d, J = 2.01 Hz), 7.51−7.56 (3H, m), 7.37 (1H, d, J = 1.76 Hz), 6.95 (1H, d, J = 1.51 Hz), 3.88 (3H, s). ^{13}C NMR (100 MHz, CH_3OD-d) δ 162.0, 153.5, 147.3, 134.7, 134.0, 129.1, 128.4, 120.0, 116.0, 115.7, 115.1, 112.0, 107.8. m/z (+ESI) calc. for $C_{15}H_{12}N_2O_4$ $(M)^-$ 284.3, found 283.0 $([M] - H)^-$.

*5-(Benzo[b]thiophene-5-ylcarbamoyl)-1-methyl-1H-pyrrole-3-carboxylic acid (**26**).* The reaction afforded 85.0 mg (7%) as brown solid (181 °C).

R_f value (acetone/DCM 80:20): 0.39; ^{1}H NMR (400 MHz, CD_3OD-d) δ 8.20 (1H, d, J = 1.76 Hz), 7.85 (1H, d, J = 8.81 Hz), 7.52−7.59 (3H, m), 7.38 (1H, J = 1.76 Hz), 7.34 (1H, d, J = 4.78 Hz), 3.99 (3H, s). ^{13}C NMR (100 MHz, CD_3OD-d) δ 141.6, 136.9, 136.5, 134.1, 128.5, 124.9, 123.4, 119.9, 116.6, 116.1, 115.8. m/z (+ESI) calc. for $C_{15}H_{12}N_2O_3S$ $(M)^-$ 300.3, found 301.0 $([M] + H)^+$.

*General Procedure Adopted for Boc-Deprotection (**18**, **19**, **22**).* The Boc-protected compound was added to a mixture of DCM (2 mL) and TFA (1 mL) and kept under a magnetic stirrer for 30 min. The organic solvent was then evaporated under vacuum.

*General Procedure for Methyl Ester Hydrolysis (**21**, **24**).* The compound bearing the methyl ester was solubilized in a mixture of H_2O (10 mL) and dioxane (2 mL), and an excess of NaOH was added. The solution was kept under magnetic stirring for 5 h until the completion of the reaction. The dioxane was then eliminated under vacuum at the rotary evaporator, and HCl was added to the aqueous solution to reach pH = 2. The product was subsequently extracted with EtOAc (50 mL), and the organic solvent was evaporated using a rotary evaporator.

*General Procedure Adopted for the Amide Coupling between PBD Core and Biaryl Moiety and for the Final Deprotection (**27**−**32**).* The moiety bearing the carboxylic acid was dissolved in DMF (4 mL), and DMAP (3 equiv) and EDCI (2 equiv) were added to the solution, which was left under a magnetic stirrer for 30 min. The amino compound was then added to the mixture, which was kept in an N_2 atmosphere and was stirred at room temperature overnight at which point TLC showed the completion of the reaction. Then, an aqueous solution of citric acid (100 mL) at pH = 2 was added, and the product was extracted with EtOAc (100 mL). The solvent was evaporated under vacuum, and the product was purified by flash column chromatography (mobile phase: from DCM, 100%, to DCM/acetone, 60:40, v/v). The compound obtained was dissolved in DCM (3 mL), and $Pd(PPh_3)_4$ (0.05 equiv), triphenylphosphine (0.25 equiv), and pyrrolidine (1.2 equiv) were added. The solution was left under a magnetic stirrer for 30 min, and then, the solvent was evaporated using a rotary evaporator. The obtained solid was kept under high vacuum for 15 min, and the product was finally purified through flash column chromatography (mobile phase: from DCM, 100%, to DCM/acetone, 40:60, v/v).

*(S)-N-(Benzofuran-5-yl)-4-(4-((7-methoxy-5-oxo-2,3,5,11a-tetrahydro-1H-benzo[e]pyrrolo[1,2-a][1,4]diazepin-8-yl)oxy)-butanamido)-1-methyl-1H-pyrrole-2-carboxamide (**27**).* The reaction afforded 38.0 mg (38%) as white solid (mp 144 °C).

R_f value (DCM/acetone 20:80): 0.25; ^{1}H NMR (400 MHz, $CDCl_3$) δ 8.19 (1H, s), 8.13 (1H, s), 7.92 (1H, d, J = 2.01 Hz), 7.62 (1H, d, J = 4.28 Hz), 7.57 (1H, d, J = 2.27 Hz), 7.47 (1H, s), 7.31−7.41 (1H, m), 7.30 (1H, m), 7.09 (1H, d, J = 1.76 Hz), 6.68 (1H, dd, J = 2.14, 0,88 Hz), 6.57 (1H, d, J = 1.76 Hz), 4.05 (2H, t, J = 6.04 Hz), 3.85 (3H, s), 3.82 (3H, s), 3.72−3.79 (1H, m), 3.64−3.69 (1H, m), 3.50−3.54 (1H, m), 2.44−2.50 (2H, m), 2.16−2.33 (4H, m), 1.95−2.06 (3H, m). ^{13}C NMR (100 MHz, $CDCl_3$) δ 168.9, 163.6, 161.8, 159.0, 150.7, 149.6, 146.6, 144.7, 139.6, 132.2, 126.73, 122.2, 120.5, 119.3, 118.6, 117.0, 112.2, 110.6, 110.3, 109.7, 105.8, 103.0, 67.0, 55.0, 52.7, 45.7, 35.7, 29.9, 28.2, 23.9, 23.1. IR (FT/IR, ν_{max}/cm^{-1}): 1600, 1468, 1433, 1263, 1200, 1228, 760, 733. HRMS (EI, m/z): calc for $C_{31}H_{31}N_5O_6$ (M), 570.2347; found, 570.2340.

*(S)-N2-(benzofuran-5-yl)-N4-(3-((7-methoxy-5-oxo-2,3,5,11a-tetrahydro-1H-benzo[e]pyrrolo[1,2-a][1,4]-diazepin-8-yl)oxy)propyl)-1-methyl-1H-pyrrole-2,4-dicarboxamide (**28**).* The reaction afforded 9.0 mg, (14%) as white solid (mp 135 °C).

DOI: 10.1021/acsinfecdis.7b00130
ACS Infect. Dis. 2018, 4, 158−174

R_f value (EtOAc/methanol 95:5): 0.23; ^{1}H NMR (400 MHz, $CDCl_3$) δ 8.18 (1H, br s), 7.95 (1H, d, J = 1.51 Hz), 7.65 (1H, d, 4.28 Hz), 7.61 (1H, d, J = 2.27 Hz), 7.52 (1H, s), 7.45 (1H, d, J = 8.81 Hz), 7.34 (1H, dd, J = 8.31, 1.51 Hz), 7.29 (1H, s), 7.15 (1H, br s), 6.83 (1H, s), 6.79 (1H, br s), 6.75 (1H, d, J = 2.01 Hz), 4.21−4.29 (1H, m), 4.11−4.18 (1H, m), 3.98 (3H, s), 3.86 (3H, s), 3.76−3.80 (1H, m), 3.53−3.72 (4H, m), 2.26−2.33 (2H, m), 1.94−2.07 (4H, m). ^{13}C NMR (100 MHz, $CDCl_3$) δ 163.9, 162.9, 159.7, 152.0, 150.5, 147.5, 145.9, 141.0, 132.9, 129.5, 127.9, 126.7, 120.6, 118.7, 117.9, 113.2, 112.3, 111.6, 111.0, 110.5, 106.9, 68.7, 56.4, 53.8, 53.7, 46.7, 37.3, 29.6, 29.3, 24.2. IR (FT/IR, ν_{max}/cm^{-1}): 1572, 1263, 1215, 1200, 1084, 1026, 760, 623. HRMS (EI, m/z): calc for $C_{31}H_{31}N_5O_6$ (M), 570.2347; found, 570.2344.

*(S)-4-(Benzofuran-5-carboxamido)-N-(3-((7-methoxy-5-oxo-2,3,5,11a-tetrahydro-1H-benzo[e]pyrrolo[1,2-a][1,4]-diazepin-8-yl)oxy)propyl)-1-methyl-1H-pyrrole-2-carboxamide (**29**).* The reaction afforded 20.0 mg (22%) as white solid (mp 139 °C).

R_f value (DCM/acetone 20:80): 0.26; ^{1}H NMR (400 MHz, $CDCl_3$) δ 8.71 (1H, s), 8.19 (1H, d, J = 1.76 Hz), 7.87 (1H, dd, J = 8.81, 1.76 Hz), 7.66 (1H, d, 2.27 Hz), 7.63 (1H, d, J = 4.53 Hz), 7.51 (1H, d, J = 8.56 Hz), 7.44 (1H, s), 7.35 (1H, d, J = 1.76 Hz), 6.79 (1H, dd, J = 2.27, 0.76 Hz), 6.72−6.77 (2H, m), 6.52 (1H, d, J = 1.76 Hz), 4.16−4.23 (1H, m), 4.06−4.10 (1H, m), 3.86 (3H, s), 3.74−3.82 (4H, m), 3.60−3.68 (2H, M), 3.49−3.56 (2H, m), 2.24−2.32 (2H, m), 1.99−2.10 (4H, m). ^{13}C NMR (100 MHz, $CDCl_3$) δ 165.0, 164.6, 162.6, 161.8, 156.5, 150.4, 147.6, 146.3, 140.6, 129.6, 127.6, 123.7, 123.5, 121.7, 120.9, 120.4, 119.3, 111.4, 110.4, 107.1, 103.6, 68.4, 55.9, 53.8, 46.7, 37.4, 36.5, 29.6, 29.3, 24.2. IR (FT/IR, ν_{max}/cm^{-1}): 1599, 1433, 1410, 1265, 1198, 1142, 812, 731, 623. HRMS (EI, m/z): calc for $C_{31}H_{31}N_5O_6$ (M), 570.2347; found, 570.2344.

*(S)-N-(Benzo[b]thiophen-5-yl)-4-(4-((7-methoxy-5-oxo-2,3,5,11a-tetrahydro-1H-benzo[e]pyrrolo[1,2-a][1,4]-diazepin-8-yl)oxy)butanamido)-1-methyl-1H-pyrrole-2-carboxamide (**30**).* The reaction afforded 60.0 mg (57%) as white solid (mp 139 °C).

R_f value (DCM/acetone 20:80): 0.28; ^{1}H NMR (400 MHz, $(CD_3)_2SO$) δ 9.93 (2H, d, J = 2.27 Hz), 8.35 (1H, d, J = 2.01 Hz), 7.90 (1H, d, J = 8.81 Hz), 7.78 (1H, d, J = 4.28 Hz), 7.74 (1H, d, J = 5.54 Hz), 7.63 (1H, dd, J = 8.69, 1.89 Hz), 7.42 (1H, d, J = 5.29 Hz), 7.33 (1H, s), 7.24 (1H, d, J = 1.76 Hz), 7.00 (1H, d, J = 1.76 Hz), 6.83 (1H, s),4.09−4.18 (1H, m), 3.99−4.08 (1H, m), 3.85 (3H, s), 3.83 (3H, s), 3.56−3.42 (1H, m), 2.45 (2H, t, J = 7.43 Hz), 2.14−2.31 (2H, m), 2.00−2.08 (2H, m), 1.87−1.96 (2H, m). ^{13}C NMR (100 MHz, $(CD_3)_2SO$) δ 168.8, 164.2, 163.3, 159.8, 150.1, 146.9, 140.5, 139.7, 136.2, 133.6, 127.9, 124.0, 122.6, 122.3, 122.0, 119.8, 118.8, 118.2, 114.4, 111.1, 110.0, 104.8, 67.7, 55.5, 53.4, 46.3, 36.2, 31.9, 28.8, 24.7, 23.6. IR (FT/IR, ν_{max}/cm^{-1}): 1620, 1595, 1261, 1198, 1157, 1020, 874, 768, 692, 581. HRMS (EI, m/z): calcd for $C_{31}H_{31}N_5O_5S_1$ (M), 586.2119; found, 586.2114.

*(S)-N2-(Benzo[b]thiophen-5-yl)-N4-(3-((7-methoxy-5-oxo-2,3,5,11a-tetrahydro-1H-benzo[e]pyrrolo[1,2-a][1,4]-diazepin-8-yl)oxy)propyl)-1-methyl-1H-pyrrole-2,4-dicarboxamide (**31**).* The reaction afforded 8.5 mg (14%) as a pale yellow solid (mp 142 °C).

R_f value (DCM/acetone 20:80): 0.26; ^{1}H NMR (400 MHz, $CDCl_3$) δ 8.26 (1H, br s), 8.24 (1H, s), 7.80 (2H, dd, J = 8.44, 5.41 Hz), 7.65 (1H, d, J = 3.53 Hz), 7.52 (1H, s), 7.40−7.47 (2H, m), 7.35 (1H, d, J = 8.06 Hz), 7.29 (1H, s), 7.19 (1H, s), 6.82 (1H, dr.s), 4.21−4.30 (1H, m), 4.08−4.18 (1H, m), 3.98 (3H, s), 3.86 (3H, s), 3.75−3.82 (2H, m), 3.51−3.69 (4H, m), 2.25−2.34 (2H, m), 1.93−2.09 (4H, m). ^{13}C NMR (100 MHz, $CDCl_3$) δ 163.9, 162.8, 160.7, 159.7, 152.0, 147.5, 140.2, 135.5, 129.9, 129.6, 128.1, 127.6, 126.6, 124.0, 122.8, 117.9, 114.8, 112.4, 111.2, 68.7, 56.4, 53.7, 46.7, 37.4, 31.8, 29.7, 29.3, 24.2, 21.7. IR (FT/IR, ν_{max}/cm^{-1}): 1599, 1572, 1431, 1024, 970, 808, 768, 694, 482. HRMS (EI, m/z): calc for $C_{31}H_{31}N_5O_5S_1$ (M), 586.2119; found, 586.2116

*(S)-4-(Benzo[b]thiophene-5-carboxamido)-N-(3-((7-methoxy-5-oxo-2,3,5,11a-tetrahydro-1H-benzo[e]pyrrolo[1,2-a][1,4]diazepin-8-yl)oxy)propyl)-1-methyl-1H-pyrrole-2-carboxamide (**32**).* The reaction afforded 57.0 mg (36%) as pale yellow solid (mp 169 °C).

R_f value (DCM/acetone 20:80): 0.28; ^{1}H NMR (400 MHz, $CDCl_3$) δ 9.27 (1H, s), 8.40 (1H, s), 7.86−7.91 (1H, m), 7.81−7.85 (1H, m), 7.58 (1H, d, J = 4.28 Hz), 7.44 (1H, d, J = 5.54 Hz), 7.38 (1H, s), 7.33 (1H, d, J = 1.76 Hz), 7.28 (1H, d, J = 5.54 Hz), 6.79 (1H, t, J = 5.54 Hz), 6.70 (1H, s), 6.56 (1H, d, J = 1.76 Hz), 4.05−4.13 (1H, m), 3,94−4.02 (1H, m), 3.78 (3H, s), 3.71 (3H, s), 3.41−3.65 (5H, m), 2,23 (2H, t, J = 6.29 Hz), 1.90−2.02 (4H, m). ^{13}C NMR (100 MHz, $CDCl_3$) δ 165.0, 164.7, 162.5, 161.8, 150.4, 147.5, 142.5, 140.5, 139.4, 130.7, 127.7, 124.3, 123.5, 123.0, 122.9, 122.4, 121.9, 120.2, 119.3, 111.3, 110.2, 103.8, 68.3, 55.9, 53.7, 46.7, 37.3, 36.4, 29.5, 29.3, 24.2. IR (FT/IR, ν_{max}/cm^{-1}): 1600, 1431, 1261, 1200, 1161, 869, 810, 694, 606, 482. HRMS (EI, m/z): calc for $C_{31}H_{31}N_5O_5S_1$ (M), 586.2119; found, 586.2113.

FRET Based DNA Melting Assay. The oligonucleotide sequence used for the FRET based DNA thermal denaturation assays was purchased from Eurogentec, Southampton, UK. Netropsin hydrochloride was purchased from Sigma-Aldrich UK. The working solution of the oligonucleotide solution (400 nM) was prepared in a FRET buffer (optimized as 50 mM potassium, 50 mM cacodylate, pH 7.4). The oligonucleotides were annealed by heating the samples to 85 °C for 6 min followed by cooling to 25 °C and storing at this temperature for 5 h. Annealed DNA (25 μL) and sample solution (25 μL) were added to each well of a 96-well plate (MJ Research, Waltham, MA), incubated for 3 h, and processed in a DNA Engine Opticon (MJ Research). Fluorescence readings were taken at intervals of 0.5 °C over the range of 30−100 °C, with a constant temperature maintained for 30 s prior to each reading. The raw data was imported into the Origin program (Version 7.0, OriginLab Corp.), and the graphs were smoothed using a 10-point running average and then normalized. The determination of melting temperatures was based on values at the maxima of the first derivative of the smoothed melting curves using a script. The difference between the melting temperature of each sample and that of the blank (ΔT_m) was used for comparative purposes.

Eukaryotic Toxicity Determination. *Cell Culture.* The HeLa (human cervical cancer) cell line was obtained from the American Type Culture Collection. The HeLa cell line was maintained in Dulbecco's Modified Eagles Media (DMEM; Invitrogen) supplemented with fetal bovine serum (10% v/v; Invitrogen), L-glutamine (2 mM; Invitrogen), nonessential amino acids (1×; Invitrogen), and penicillin−streptomycin (1% v/v, Invitrogen). For WI-38, high glucose DMEM (4.5 g/L; Invitrogen), fetal bovine serum (10%, Biosera UK), non-essential amino acids (1×; Invitrogen), and L-glutamine (2 mM; Invitrogen) were used for subculturing. During seeding, cells were counted using a Neubauer hemocytometer (Assistant, Germany) by microscopy (Nikon, USA) on a

DOI: 10.1021/acsinfecdis.7b00130
ACS Infect. Dis. 2018, 4, 158−174

nonadherent suspension of cells that were washed in PBS, trypsinized, centrifuged at 8 °C at 8000 rpm for 5 min, and resuspended in a fresh medium.

MTT Assay. The cells were grown in normal cell culture conditions at 37 °C in a 5% CO_2 humidified atmosphere using the cell-specific medium listed in the cell culture section above. The cell count was adjusted to 10^5 cells/mL, and 10 000 cells were added per well. The cells were incubated for 24 h, and 1 μL of the appropriate ligand concentration was added to the wells in triplicate. After 24 h of continuous exposure to each compound, the cell viability was determined using the 3-(4,5-dimethylthiazol-2-yl)-2,5-diphenyltetrazolium bromide (MTT) (Lancaster Synthesis Ltd., UK) colorimetric assay. Absorbance was quantified by spectrophotometry at λ = 570 nm (Envision Plate Reader, PerkinElmer, USA). Percentage survival values were calculated by a dose−response analysis using the GraphPad Prism software.

Microbiological Evaluation. *Minimum Inhibitory Concentration (MIC).* The MIC is the lowest concentration of an antimicrobial that will inhibit the growth of 99% of a microorganism after overnight incubation. The MIC of the synthesized compounds was determined using the broth microdilution method. Bacteria were grown in Tryptic Soy Broth (TSB) (Sigma) or on Tryptic Soy Agar (TSA) plates at 37 °C. A solution of 128 μg/mL of the synthesized molecules in water was prepared from a 2 mg/mL stock solution in DMSO and then sequentially diluted by 2-fold in a 96 well plate. 100 μL of bacterially infected media at a concentration of 1× 10^6 CFU/mL was inoculated in each well (final bacterial conc. of 5 × 10^5 CFU/mL). The maximum DMSO content in each well after the addition of the media was ≤1%. The plate was then incubated statically at 37 °C for 20 h, and absorbance at a wavelength of 600 nm (OD_{600}) was measured.

Time-Kill Kinetics Assay. The bactericidal or bacteriostatic mode of killing was analyzed using a time-kill assay. Briefly, 10 mL of bacteria at a starting concentration of approximately 10^6 CFU/mL was incubated in a glass conical flask in TSB for 24 h at 37 °C with shaking in the presence of the compound at 4× MIC. At specified time-points, 100 μL was removed from the culture and diluted in PBS using the method of Miles et al.[33] 10 μL spots of the dilutions were plated onto TSA plates and incubated overnight at 37 °C to obtain a cell count.

Gyrase Inhibition Assay. The wild-type gyrase and the gyrase with the S84L mutation were treated with compound **29** and the positive control ciprofloxacin using the cell-free *S. aureus* gyrase supercoiling high throughput plate assay (#SATRG01), obtained from Inspiralis (Norwich, UK).[34] This assay is based on the fact that negatively supercoiled plasmids form intermolecular triplex DNA more readily than relaxed plasmids under the experimental condition. The methods were conducted as per the manufacturer's instructions as described previously.[35] Briefly, a relaxed pNO1, a modified form of pBR322 which contains a "triplex-forming sequence", was used as the substrate. Initially, the wells were hydrated using 1× wash buffer (20 mM Tris·HCl (pH 7.6), 137 mM NaCl, 0.005% (w/v) bovine serum albumin (acetylated), 0.05% (v/v) Tween-20). This was followed by immobilization of 100 μL of 500 nM TFO1 oligo in each well by incubating for 5 min at room temperature. Excess oligo was carefully washed with assay buffer and ultrapure water. Twenty-four μL of mix buffer was prepared by adding 0.75 μL of pNO1, 6 μL of assay buffer (40 mM HEPES, KOH, 10 mM magnesium acetate, 10 mM DTT, 2 mM ATP, 500 mM potassium glutamate, 0.05 mg/mL albumin, pH 7.6), and 17.25 μL of ultrapure water. The mix buffer was added to each well. This was followed by addition of 3 μL of inhibitor and 3 μL of dilution buffer (50 mM Tris·HCl, 1 mM DTT, 1 mM EDTA, 40% (w/v) glycerol). The plate was incubated at 37 °C for 30 min. This was followed by the addition of 100 μL of TF (triplex forming) assay buffer (10 mM sodium acetate, pH 4.7, 50 mM sodium chloride, and 50 mM magnesium chloride) and incubating the plate for a further period of 30 min to allow triplex formation. The wells were washed with 200 μL of TF buffer to remove the unbound plasmid. Finally, PR omega diamond dye (in 10 mM Tris-HCl, pH 8, 1 mM EDTA) was added, and the plates were read by a fluorescent plate reader (ex. 495−15, em. 537−20) after 20 min of incubation at room temperature in the dark.

Molecular Modeling. *Preparation of DNA and Compounds Structures.* Double strand (DS) DNA type B (BDNA) was generated by the NAB module of the AMBER 12.0 package program, using the template of the sequences used in the study (AT-rich 5′-TATATAAGATATATATA-3′, mixed 5′-TAG-CTAGCTAGCTAGCG-3′, and GC-rich 5′-GCGCGCGC-GCGGCGCGC-3′). PDB files for the ligands were generated by Chem3DPro 13.0. DNA and compounds' structures were minimized by SYBYL software before covalent molecular docking.

Covalent Molecular Docking. Covalent docking was performed by forming the covalent bond between the exocyclic amine of guanine and the N10−C11 imine of the PBD using the Autodock SMINA.[36] C11-*S*-stereochemistry was maintained in every case at the binding interface of the PBD. All parameters were kept at their default values.

Molecular Dynamics (MD) Simulations. After covalent molecular docking, the best poses of each complex were selected as the starting structures to run MD simulations for 10 ns. The MD simulations were carried out using the AMBER 12.0 package program. The force fields parameters for the compounds were generated using the ANTECHAMBER module of AMBER program. Each system was solvated by using an octahedral box of TIP3P water molecules. Periodic boundary conditions and the particle-mesh Ewald (PME) method were employed in all the simulations.[37] During each simulation, all bonds in which the hydrogen atom was present were considered fixed, and all other bonds were constrained to their equilibrium values by applying the SHAKE algorithm.[38] A cutoff radius of 12 Å was used for the systems. Minimization was performed in two phases, and each phase was performed in two stages. In the first phase, ions and all water molecules were minimized for 500 cycles of the steepest descent followed by 500 cycles of conjugate gradient minimization. Afterward, the whole systems were minimized for a total of 1000 cycles without restraint wherein 500 cycles of steepest descent were followed by 500 cycles of conjugate gradient minimization. After minimizations, the systems were heated for 100 ps while the temperature was raised from 0 to 300 K, and then, equilibration was performed without a restraint for 100 ps while the temperature was kept at 300 K. Sampling of reasonable configurations was conducted by running a 10 ns simulation with a 2 fs time step at 300 K and 1 atm pressure. A constant temperature was maintained by applying the Langevin algorithm while the pressure was controlled by the isotropic position scaling protocol used in AMBER.[39]

MM-PBSA/MM_GBSA Calculation. Twenty snapshots were collected from the last 200 ps of simulations of DNA−compound complexes for postprocessing analysis. The ΔG_{PB}

DOI: 10.1021/acsinfecdis.7b00130
ACS Infect. Dis. 2018, 4, 158−174

term was calculated by solving the finite-difference Poisson−Boltzmann equation using the internal PBSA program.[40] The SCALE value was set to 2. The Parse radii were employed for all atoms. The solvent probe radius was set at 1.4 Å (with the radii in the prmtop files). MM-PBSA running was performed with the pbsa module (PROC = 2). The value of the exterior dielectric constant was set at 80, and the solute dielectric constant was set at 1.[41] The nonpolar contribution was determined on the basis of the solvent accessible surface area (SASA) using the LCPO method[42] and CAVITY-OFFSET set at 0.00.

Molecular Docking of the Compounds to Wild and Mutant Gyrase A. AutoDock SMINA was used for molecular docking of ciprofloxacin, as a control, and compound **29** to the minimized crystal structure of gyrase A from *S. aureus* (PDB ID code 2XCT), for finding the best binding pocket by exploring all probable binding cavities in the enzyme. All the parameters were kept in their default values. Then, GOLD molecular docking was used for molecular docking of the compounds into the SMINA-located binding site for performing flexible molecular docking and determining more precise and evaluated energies and scores. On the basis of the fitness function score and ligand binding position, the best-docked pose for each compound was selected. The high fitness function score, generated using the GOLD program, with a low binding energy value, reveals the best-docked pose for each system.

In this study, molecular docking of the compounds to the mutant form of gyraseA was performed as well. After altering Ser84 to Leu with a proper rotamer using PyMOL software, the new structure of gyraseA_S84L was minimized by using Sybyl program. For minimization, the method was set to Pawell, initial optimization was set to Simplex, termination was set to Gradient 0.01 kcal/(mol·A), and the maximum interactions were set to 10 000. The minimized structure of the mutant enzyme was used to run the molecular docking by GOLD, as explained above, for the wild-type. A genetic algorithm (GA) is used in GOLD ligand docking to thoroughly examine the ligand conformational flexibility along with the partial flexibility of the protein. The maximum number of runs was set to 20 for each compound, and the default parameters were selected (100 for the population size, 5 for the number of islands, 100 000 for the number of operations, and 2 for the niche size). Default cutoff values of 2.5 Å (dH-X) for hydrogen bonds and 4.0 Å for van-der-Waals distance were employed. When the top solutions attained the RMSD values within 1.5 Å, the GA docking was terminated.

■ ASSOCIATED CONTENT

Supporting Information

The Supporting Information is available free of charge on the ACS Publications website at DOI: 10.1021/acsinfecdis.7b00130.

Dynamic light scattering, purity data, *in silico* screening method, molecular docking, interactions with DNA gyrase, molecular models, NMR spectra, and HRMS data (PDF)

■ AUTHOR INFORMATION

Corresponding Authors

*E-mail k.miraz.rahman@kcl.ac.uk (K.M.R.).
*E-mail: mark.sutton@phe.gov.uk (J.M.S.).

ORCID

Khondaker Miraz Rahman: 0000-0001-8566-8648

Author Contributions

⊥P.A. and C.K.H. contributed equally to the manuscript.

Notes

The authors declare no competing financial interest.

■ ACKNOWLEDGMENTS

We gratefully acknowledge the support provided by the High-Performance Compute Cluster (HPC) of King's College London (Ada) and Dr Stuart Jones for his help with the dynamic light scattering experiment. We are thankful to Erasmus+ research funding scheme for providing a scholarship to P.A., and BBSRC (Sparking Impact Award) and Public Health England for supporting this work (Award codes JGALAQR, JGALAVR).

■ ABBREVIATIONS

PBD, pyrrolobenzodiazepine; MDR, multidrug resistant; MRSA, methicillin resistant *S. aureus*; VRE, vancomycin resistant *Enterococci*; HBTU, 2-(1*H*-benzotriazol-1-yl)-1,1,3,3-tetramethyluronium hexafluorophosphate; DIPEA, *N*,*N*-diisopropylethylamine; FRET, fluorescence resonance energy transfer; FAM, 6-carboxyfluorescein; TAMRA, 5-carboxytetramethylrhodamine; mp, melting point

■ REFERENCES

(1) Ventola, C. L. (2015) The antibiotic resistance crisis: part 1: causes and threats. *Phar. Ther. 40*, 277.

(2) Laxminarayan, R., Duse, A., Wattal, C., Zaidi, A. K., Wertheim, H. F., Sumpradit, N., Vlieghe, E., Hara, G. L., Gould, I. M., and Goossens, H. (2013) Antibiotic resistance—the need for global solutions. *Lancet Infect. Dis. 13*, 1057−1098.

(3) Rice, L. B. (2008) Federal funding for the study of antimicrobial resistance in nosocomial pathogens: no ESKAPE. *J. Infect. Dis. 197*, 1079−1081.

(4) McGowan, J. E., Jr. (2001) Economic impact of antimicrobial resistance. *Emerging Infect. Dis. 7*, 286−292.

(5) Giske, C. G., Monnet, D. L., Cars, O., and Carmeli, Y. (2008) Clinical and economic impact of common multidrug-resistant gram-negative bacilli. *Antimicrob. Agents Chemother. 52*, 813−821.

(6) Eliopoulos, G. M., Cosgrove, S. E., and Carmeli, Y. (2003) The impact of antimicrobial resistance on health and economic outcomes. *Clin. Infect. Dis. 36*, 1433−1437.

(7) Roca, I., Akova, M., Baquero, F., Carlet, J., Cavaleri, M., Coenen, S., Cohen, J., Findlay, D., Gyssens, I., Heure, O., et al. (2015) The global threat of antimicrobial resistance: science for intervention. *New Microbes New Infect. 6*, 22−29.

(8) Silver, L. L. (2011) Challenges of antibacterial discovery. *Clin. Microbiol. Rev. 24*, 71−109.

(9) Boucher, H. W., Talbot, G. H., Bradley, J. S., Edwards, J. E., Gilbert, D., Rice, L. B., Scheld, M., Spellberg, B., and Bartlett, J. (2009) Bad bugs, no drugs: no ESKAPE! An update from the Infectious Diseases Society of America. *Clin. Infect. Dis. 48*, 1−12.

(10) Fischbach, M. A., and Walsh, C. T. (2009) Antibiotics for emerging pathogens. *Science 325*, 1089−1093.

(11) Antonow, D., and Thurston, D. E. (2011) Synthesis of DNA-interactive pyrrolo[2,1-c][1,4]benzodiazepines (PBDs). *Chem. Rev. 111*, 2815−2864.

(12) Gerratana, B. (2012) Biosynthesis, synthesis, and biological activities of pyrrolobenzodiazepines. *Med. Res. Rev. 32*, 254−293.

(13) Mantaj, J., Jackson, P. J. M., Rahman, K. M., and Thurston, D. E. (2017) From Anthramycin to Pyrrolobenzodiazepine (PBD)-Containing Antibody−Drug Conjugates (ADCs). *Angew. Chem., Int. Ed. 56*, 462−488.

DOI: 10.1021/acsinfecdis.7b00130
ACS Infect. Dis. 2018, 4, 158−174

(14) Rahman, K. M., James, C. H., Bui, T. T., Drake, A. F., and Thurston, D. E. (2011) Observation of a single-stranded DNA/pyrrolobenzodiazepine adduct. *J. Am. Chem. Soc. 133*, 19376−19385.
(15) Thurston, D. E., Bose, D. S., Thompson, A. S., Howard, P. W., Leoni, A., Croker, S. J., Jenkins, T. C., Neidle, S., Hartley, J. A., and Hurley, L. H. (1996) Synthesis of sequence-selective C8-linked pyrrolo [2, 1-c][1, 4] benzodiazepine DNA interstrand cross-linking agents. *J. Org. Chem. 61*, 8141−8147.
(16) Leimgruber, W., Stefanović, V., Schenker, F., Karr, A., and Berger, J. (1965) Isolation and characterization of anthramycin, a new antitumor antibiotic. *J. Am. Chem. Soc. 87*, 5791−5793.
(17) Hertzberg, R. P., Hecht, S. M., Reynolds, V. L., Molineux, I. J., and Hurley, L. H. (1986) DNA-sequence specificity of the pyrrolo 1,4 benzodiazepine antitumor antibiotics - Methidiumpropyl-EDTA-iron-(ii) footprinting analysis of DNA-binding sites for anthramycin and related drugs. *Biochemistry 25*, 1249−1258.
(18) Hurley, L. H., Reck, T., Thurston, D. E., Langley, D. R., Holden, K. G., Hertzberg, R. P., Hoover, J. R. E., Gallagher, G., Faucette, L. F., Mong, S. M., and Johnson, R. K. (1988) Pyrrolo 1,4 benzodiazepine antitumor antibiotics - relationship of DNA alkylation and sequence specificity to the biological-activity of natural and synthetic compounds. *Chem. Res. Toxicol. 1*, 258−268.
(19) Puvvada, M. S., Forrow, S. A., Hartley, J. A., Stephenson, P., Gibson, I., Jenkins, T. C., and Thurston, D. E. (1997) Inhibition of bacteriophage T7 RNA polymerase in vitro transcription by DNA-binding pyrrolo 2,1-c 1,4 benzodiazepines. *Biochemistry 36*, 2478−2484.
(20) Rahman, K. M., Vassoler, H., James, C. H., and Thurston, D. E. (2010) DNA Sequence Preference and Adduct Orientation of Pyrrolo[2,1-c][1,4]benzodiazepine Antitumor Agents. *ACS Med. Chem. Lett. 1*, 427−432.
(21) Hartley, J. A., Spanswick, V. J., Brooks, N., Clingen, P. H., McHugh, P. J., Hochhauser, D., Pedley, R. B., Kelland, L. R., Alley, M. C., Schultz, R., et al. (2004) SJG-136 (NSC 694501), a novel rationally designed DNA minor groove interstrand cross-linking agent with potent and broad spectrum antitumor activity. *Cancer Res. 64*, 6693−6699.
(22) Rosado, H., Rahman, K. M., Feuerbaum, E.-A., Hinds, J., Thurston, D. E., and Taylor, P. W. (2011) The minor groove-binding agent ELB-21 forms multiple interstrand and intrastrand covalent cross-links with duplex DNA and displays potent bactericidal activity against methicillin-resistant *Staphylococcus aureus*. *J. Antimicrob. Chemother. 66*, 985−996.
(23) Antonow, D., and Thurston, D. E. (2011) Synthesis of DNA-interactive pyrrolo [2, 1-c][1, 4] benzodiazepines (PBDs). *Chem. Rev. 111*, 2815−2864.
(24) Rahman, K. M., Rosado, H., Moreira, J. B., Feuerbaum, E.-A., Fox, K. R., Stecher, E., Howard, P. W., Gregson, S. J., James, C. H., de la Fuente, M., Waldron, D. E., Thurston, D. E., and Taylor, P. W. (2012) Antistaphylococcal activity of DNA-interactive pyrrolobenzodiazepine (PBD) dimers and PBD-biaryl conjugates. *J. Antimicrob. Chemother. 67*, 1683−1696.
(25) Rahman, K. M., Jackson, P. J., James, C. H., Basu, B. P., Hartley, J. A., de la Fuente, M., Schatzlein, A., Robson, M., Pedley, B., Pepper, C., et al. (2013) C8-linked pyrrolobenzodiazepine (PBD)-biaryl conjugates with femtomolar in vitro cytotoxicity and in vivo antitumour activity in mouse models of pancreatic and breast cancer. *Cancer Res. 73*, 1129.
(26) Kotecha, M., Kluza, J., Wells, G., O'Hare, C. C., Forni, C., Mantovani, R., Howard, P. W., Morris, P., Thurston, D. E., Hartley, J. A., et al. (2008) Inhibition of DNA binding of the NF-Y transcription factor by the pyrrolobenzodiazepine-polyamide conjugate GWL-78. *Mol. Cancer Ther. 7*, 1319−1328.
(27) Rahman, K. M., Jackson, P. J., James, C. H., Basu, B. P., Hartley, J. A., de la Fuente, M., Schatzlein, A., Robson, M., Pedley, R. B., Pepper, C., et al. (2013) GC-targeted C8-linked pyrrolobenzodiazepine−biaryl conjugates with femtomolar in vitro cytotoxicity and in vivo antitumor activity in mouse models. *J. Med. Chem. 56*, 2911−2935.
(28) Tiberghien, A. C., Evans, D. A., Kiakos, K., Martin, C. R., Hartley, J. A., Thurston, D. E., and Howard, P. W. (2008) An asymmetric C8/C8′-tripyrrole-linked sequence-selective pyrrolo [2, 1-c][1, 4] benzodiazepine (PBD) dimer DNA interstrand cross-linking agent spanning 11 DNA base pairs. *Bioorg. Med. Chem. Lett. 18*, 2073−2077.
(29) Renčiuk, D., Zhou, J., Beaurepaire, L., Guédin, A., Bourdoncle, A., and Mergny, J.-L. (2012) A FRET-based screening assay for nucleic acid ligands. *Methods 57*, 122−128.
(30) Gregson, S. J., Howard, P. W., Hartley, J. A., Brooks, N. A., Adams, L. J., Jenkins, T. C., Kelland, L. R., and Thurston, D. E. (2001) Design, synthesis, and evaluation of a novel pyrrolobenzodiazepine DNA-interactive agent with highly efficient cross-linking ability and potent cytotoxicity. *J. Med. Chem. 44*, 737−748.
(31) Mosmann, T. (1983) Rapid colorimetric assay for cellular growth and survival: application to proliferation and cytotoxicity assays. *J. Immunol. Methods 65*, 55−63.
(32) Kamal, A., Ramesh, G., Laxman, N., Ramulu, P., Srinivas, O., Neelima, K., Kondapi, A. K., Sreenu, V., and Nagarajaram, H. (2002) Design, synthesis, and evaluation of new noncross-linking pyrrolobenzodiazepine dimers with efficient DNA binding ability and potent antitumor activity. *J. Med. Chem. 45*, 4679−4688.
(33) Miles, A. A., Misra, S., and Irwin, J. (1938) The estimation of the bactericidal power of the blood. *J. Hyg. 38*, 732−749.
(34) Maxwell, A., Burton, N. P., and O'Hagan, N. (2006) High-throughput assays for DNA gyrase and other topoisomerases. *Nucleic Acids Res. 34*, e104.
(35) Picconi, P., Hind, C., Jamshidi, S., Nahar, K., Clifford, M., Wand, M. E., Sutton, J. M., and Rahman, K. M. (2017) Triaryl Benzimidazoles as a New Class of Antibacterial Agents against Resistant Pathogenic Microorganisms. *J. Med. Chem. 60*, 6045−6059.
(36) Koes, D. R., Baumgartner, M. P., and Camacho, C. J. (2013) Lessons learned in empirical scoring with smina from the CSAR 2011 benchmarking exercise. *J. Chem. Inf. Model. 53*, 1893−1904.
(37) Darden, T., York, D., and Pedersen, L. (1993) Particle Mesh Ewald - an N.Log(N) Method for Ewald Sums in Large Systems. *J. Chem. Phys. 98*, 10089−10093.
(38) Ryckaert, J. P., Ciccotti, G., and Berendsen, H. J. C. (1977) Numerical-Integration of Cartesian Equations of Motion of a System with Constraints - Molecular-Dynamics of N-Alkanes. *J. Comput. Phys. 23*, 327−341.
(39) Case, D. A., Cheatham, T. E., Darden, T., Gohlke, H., Luo, R., Merz, K. M., Onufriev, A., Simmerling, C., Wang, B., and Woods, R. J. (2005) The Amber biomolecular simulation programs. *J. Comput. Chem. 26*, 1668−1688.
(40) Case, D. A., Darden, T. A., Cheatham, T. E., Simmerling, C. L., Wang, J., Duke, R. E., Luo, R., Walker, R. C., Zhang, W., Merz, K. M., Roberts, B., Hayik, S., Roitberg, A., Seabra, G., Swails, J., Götz, A. W., Kolossváry, I., Wong, K. F., Paesani, F., Vanicek, J., Wolf, R. M., Liu, J., Wu, X., Brozell, S. R., Steinbrecher, T., Gohlke, H., Cai, Q., Wang, X., Ye, J., Hsieh, M.-J., Cui, G., Roe, D. R., Mathews, D. H., Seetin, M. G., Salomon-Ferrer, R., Sagui, C., Babin, V., Luchko, T., Gusarov, S., Kovalenko, A., and Kollman, P. A. (2012) *AMBER 12*, University of California, San Francisco.
(41) Wang, W., and Kollman, P. A. (2000) Free energy calculations on dimer stability of the HIV protease using molecular dynamics and a continuum solvent model. *J. Mol. Biol. 303*, 567−582.
(42) Weiser, J., Shenkin, P. S., and Still, W. C. (1999) Approximate atomic surfaces from linear combinations of pairwise overlaps (LCPO). *J. Comput. Chem. 20*, 217−230.

DOI: 10.1021/acsinfecdis.7b00130
ACS Infect. Dis. 2018, 4, 158−174